Deanship of Graduate Studies

Al-Quds University

Spectroscopic Study of the Interaction of Vitamin K_1(Phylloquinone) with Human Serum Albumin (HSA)

Ola Fahed Jameel Hourani

M.Sc. Thesis

Jerusalem – Palestine

1434 / 2013

Spectroscopic Study of the Interaction of Vitamin K_1 (Phylloquinone) with Human Serum Albumin (HSA)

Prepared by:

Ola Fahed Jameel Hourani

B.Sc. Physics, Al-Quds University, Palestine

Supervisor: Dr. Musa Abu Teir

Co- supervisor: Prof. Mahmoud Abu- hadid

"A thesis Submitted to the Faculty of Science and Technology, Al-Quds University in Partial Fulfillment of the Requirements for the Degree of Master of Science in Physics"

1434 / 2013

Deanship of Graduate Studies

Al-Quds University

Physics Department

Thesis Approval

Spectroscopic study of the interaction of Vitamin K_1(Phylloquinone) with Human Serum Albumin (HSA)

Prepared by: Ola Fahed Jameel Hourani

Registration No: 20920226

Supervisor: Dr. Musa Abu Teir

Prof. Mahmoud Abu- hadid

Master thesis submitted and accepted, Date: /   /2013

The names and signatures of the examining committee members are as follows:

1-Head of Committee: .... Signature: ....

2-Internal Examiner: .... Signature: ....

3-External Examiner: Dr. jamal Ghabboun Signature: ....

4-Committee member: .... Signature: ....

Jerusalem – Palestine

1434 / 2013

Dedication

I Dedicate this thesis to my beloved family for their endless support and encouragement in my life: especially to my mother for her encouragement, I would not be who I am today without her love and support during the difficult and tiring times.

Also I dedicate my work to my husband Hamzah; who has been a source of motivation and strength during moments of despair, who taught me to be patient and perform the most difficult things step by step, Many thanks for his prayers and asking Allah to help me.

I will not forget to thank my best friend shurrok, my sisters and my friends whom were like sisters, Haleemah and Aseel for their encouragement during my work

Ola Fahed Jameel Hourani

Declaration

I declare that this thesis is my own work under the supervision of Dr. Musa Abu Teir and Prof. Mahmoud Abu-hadid. This thesis contains no material previously published except where due references is made, and it is submitted for the degree of master at Al-Quds University.

Ola FahedJameelHourani

Acknowledgements

Firstly, great of thanks to Allah, who helped me to finish this thesis, I felt his presence beside me during these difficult times.

This thesis would not have been possible without the support of many peoples, many thanks to my advisors; Dr. Musa Abu Teir and Prof. Mahmoud Abu-hadid, whom helped me to achieve my dream to work in Biophysics field and for their help and encouragements during my work.

Also I want to thank Dr. SaqerDarwish for his help, and Mr. JafarGithan, who helped me to be able to deal with the instruments in Biophysics Lab.

Lot of thanks for the Nano-Technology Lab group; Maryam, Abeer and Leena for their help and encouragements.

ABSTRACT

The absorption, distribution and metabolism of many molecules can be altered based on their affinity to Human Serum Albumin (HSA). HSA is often increases the apparent solubility of hydrophobic ligands in plasma and modulate their delivery to cells. In this study, the interaction between vitamin K_1 and HSA has been investigated using Ultraviolet and Visible (UV-VIS) absorption spectrophotometry and Fourier Transform Infrared (FTIR) spectroscopy; binding constant and the effects on the protein secondary structure have been provided. From UV-VIS absorption spectrophotometry which showed an increase in the absorption intensity with increasing the molecular ratios of vitamin$K_1$to HSA, it is found that the value of the binding constant forvitaminK_1:HSA is , K equals 60 M^{-1}. When FTIR spectroscopy is used in the mid infrared region with fourier self deconvolution, second derivative, difference spectra, peak piking and curve fitting were used to determine the effect of vitamin K_1 on the protein secondary structure in the amides (I, II and III) regions. From the FTIR absorbance spectra, it is found that the intensity of the absorption bands increased with increasing the molecular ratios of vitaminK_1. Furthermore from the deconvolved and curve fitted spectra, it is found that the absorbance intensity for α- helices increases relative to β- sheets; this increase in intensity is related to the formation of H- bonding between the vitamin and the protein.

Table of contents

List of Tables

List of figures

x

List of abbreviations

Symbol	Abbreviation representation
HSA	Human Serum Albumin
UV-VIS	Ultraviolet and Visible
NMR	Nuclear Magnetic Resonance
FTIR	Fourier Transform Infrared
Trp	Tryptophan
Nm	Nanometer
Cys	Cystine
MCT	Mercurt Cadmium Telluride
OPUS	Optical User Software
ZPD	Zero Path Difference
MO	Molecular Orbital
HOMO	The Highest Occupied Molecular Orbital
LUMO	The Lowest Unoccupied Molecular Orbital
KDa	Kilodalton
ND	NanoDrop
CCD	A Charge-Coupled Device
PC	Personal Computer
μL	Micro Liter
LED	Light Emitting Diode
MIR	Mid Infrared
FSD	Fourier Self Deconvolution
Si	Silicon
Ge	Germanium
InSb	Indium antimonide
IIR-DLATGS	Deuterated l-alanine-doped triglycin sulfate
InGaAs	Indium-Gallium-Arsenide.

List of Symbols

Symbol	Description
E_p	Photon energy
H	Planck's constant
E_{total}	Total energy
$E_{electronic}$	Electronic energy
$E_{vibrational}$	Vibrational energy
$E_{rotational}$	Rotational energy
$E_{translational}$	Translational energy
C	Speed of light
μ	Reduced mass
r_{eq}	Equilibrium distance
H	Hamiltonian
D_{eq}	Dissociation energy
Eq	Equation
$\overline{\omega}_e$	Oscillation frequency
χ_e	The anharmonicity constant
$G_{\circ}$	Constant that arises partly from anharmonicity and partly From the vibration-rotation interaction
T	Transmittance
A	Absorbance
$I(\tilde{v})$	Intensity of the transmitted IR energy
$I_{\circ}(\tilde{v})$	Intensity of irradiating IR energy
$a_i(\tilde{v})$	The linear absorption coefficient
b	The thickness of the sample
c_i	The concentration at component i
λ	The radiation wavelength
ν	The radiation frequency
$\tilde{v}$	The radiation wavenumber
δ	The optical path difference
Δ	The distance that the mirror moving away from the beam splitter
K	The binding constant
F(x)	The interference record
$\mathcal{F}$	The Fourier Transform
D(x)	Dirac delta function
ψ	Wave function
$A_{\circ}$	The initial absorption of the free protein
A_{∞}	The final absorption of the ligated protein

Chapter One

Introduction

Chapter one

Introduction

HSA is the most abundant protein constituent of blood plasma (Wang, et al., 2008; Tuan, et al., 2001). It has multiple binding sites; this property gives it an exceptional ability to interact with many organic and inorganic molecules, making it as a sobulizer and transporter for many materials such as drugs, metabolites, fatty acids and metal ions (N'soukpoe-Kossi, et al., 2006; Tian, et al, 211; Stan, et al, 2009; Wang, et al., 2008). Vitamin K_1 is a hydrophobic vitamin (Gropper, et al., 2009); so it can bind to two hydrophobic pockets within HSA (Tajmir-Riahi, 2006)

The interaction between HSA and many ligands such as drugs, vitamin A, and vitamin B_{12} were studied using several types of spectroscopy such as Ultraviolet Visible (UV-VIS) spectroscopy, Nuclear Magnetic Resonance (NMR) spectroscopy, fluorescence spectroscopy, and Fourier Transform Infrared (FTIR) spectroscopy (N'soukpoe-Kossi, et al., 2006; Tian, et al, 2011; Stan, et al, 2009; Wang, et al., 2008; Ouameur, et al., 2005). In my work I study the interaction between HSA and Vitamin K_1 using UV-VIS absorption spectrophotometry and FTIR absorption spectroscopy.

1.1 Vitamins

Vitamins are low molecular weight organic components of the diet required by the organisms in very small amounts to perform specific cellular functions. They are not synthesized by the organism, so it must be ingested with the diet or obtained in some other way (Champe, et al., 1994; Gropper, et al., 2009; Friedrich, 1988).

Vitamins as shown in (Figure.1.1), are divided according to their function and their solubility into two types; hydrophilic and hydrophobic vitamins (Champe, et al., 1994).

```
                            ┌─────────────┐
                            │  Vitamins   │
                            └──────┬──────┘
                ┌──────────────────┴──────────────────┐
                ▼                                      ▼
    ┌───────────────────────┐            ┌───────────────────────┐
    │ Fat–soluble vitamins  │            │ Water–soluble vitamins│
    └───────────────────────┘            └───────────────────────┘
```

Fat–soluble vitamins

- Vitamin A (retinol, β- carotenes)
- Vitamin D (cholecalciferol)
- Vitamin K (phylloquinones,menaquinones)
- Vitamin E (tocopherols)

Water–soluble vitamins

B- Complex

Non-B- Complex

- Ascorbic acid (Vitamin C)

Energy- releasing

- Thiamin (Vitamin B_1)
- Riboflavin (Vitamin B_2)
- Niacin (Vitamin B_3)
- Biotin
- Pantothenic acid

Hematopoietic

- Folic acid
- Vitamin B_{12}

Other

- Pyridoxine (Vitamin B_6)
- Pyridoxal
- Pyridoxamine

Fig 1.1: Water and Fat soluble vitamins (Champe, et al., 1994).

Hydrophilic- vitamins are nine vitamins which are soluble in water. Where Hydrophobic- vitamins are four vitamins soluble in fat, and they are released, absorbed, and transported with the fat in the diet (Gropper, et al., 2009).The fat –soluble vitamins and their most important forms and physiological functions are described in (Table.1.1) (Combs, 2008; Friedrich, 1988).

Table 1.1: Fat –soluble vitamins with most important forms and physiological functions.

Vitamin group	Most important representative	Important active compounds	Physiological function
Vitamin A	Retinol	Retinol Retinal Retinoic acid 3-dehydroretenol	Visual pigments, epithelial cell differentiation
Provitamin A	β- carotene	α-, β- and γ- carotene β- apocarotenoids cryptoxanthine echinenone	
Vitamin D	Cholecalciferol	Ergocalciferol Cholecalciferol	Calcium homeostasis, bone metabolism
Vitamin E	α- tocopherol	α-, β-, γ-, and δ-tocotrienol	Membrane antioxidant
Vitamin K	Phylloquinone	Phylloquinone (K_1) Menaquinone (K_2) Menadione (K_3)	Blood clotting, calcium metabolism

Vitamin K is a Fat- soluble vitamin which was named from the word Koagulation which is the German spelling for coagulation (Benzakour, et al., 2008). Vitamin K functions as a coenzyme and is involved in the synthesis of a number of proteins involved in blood clotting and bone metabolism (Damon, et al., 2005; Peterson, et al., 2002).

Compounds with vitamin K activity all have a 2-methyl 1, 4-naphthoquinone ring which is shown in (Fig. 1.2.a) and a side chain at the 3-position. In nature, this 3-substituent has an isoprenoid structure with varying lengths and degrees of saturation depending on the organism by which it is synthesized. Phylloquinone (2-methyl 3-phytyl 1,4-naphthoquinone) is isolated from green plants where Menaquinones is generally are synthesized by bacteria; Phylloquinone and Menaquinone formerly were designated K_1 and K_2, respectively with a chemical structure shown in (Fig. 1.2.b) and in (Fig. 1.2.c) respectively (Gropper, et al., 2009; Benzakour, et al., 2008).

.
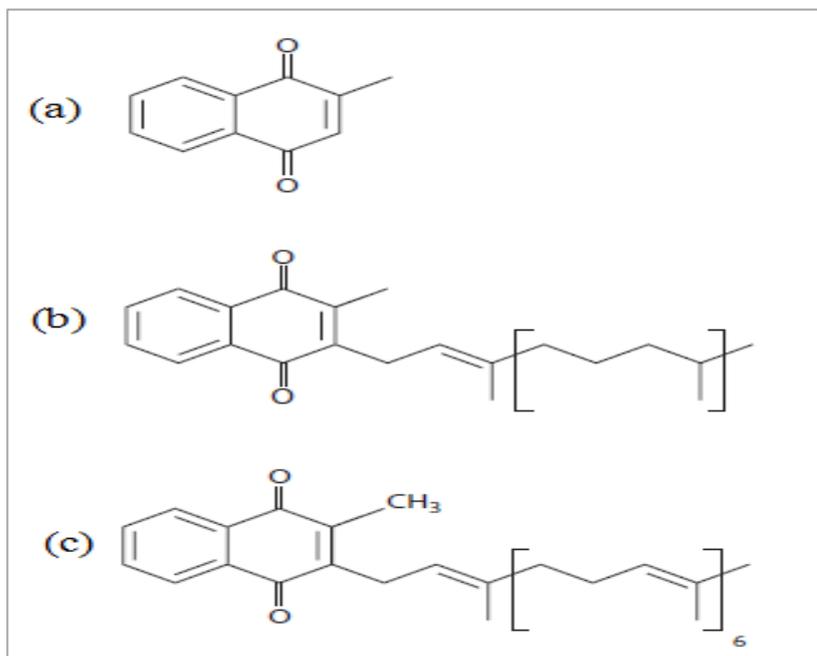
Fig 1.2: Chemical structure for (a) 2-methyl 1, 4-naphthoquinone ring, (b) Phylloquinone, (c) Menaquinone (Gropper, et al., 2009).

Phylloquinone and menaquinones are natural forms of vitamin K that are important cofactors in blood- clotting factors (Usui, et al., 1990). Phylloquinone is the predominant form of vitamin K (Thane, et al., 2002). and is provided mainly by plant foods, especially leafy green vegetables, and certain legumes (Suttie, et al., 1988).

All vitamins are now produced commercially. The commercial production of vitamins is primarily by chemical synthesis. Fat soluble vitamins are also commercially isolated from natural sources; the commercial form for phylloquinone is shown in (Fig.1.3) (Friedrich, 1988).

Fig 1.3: Commercial form of vitamin K_1 (Phylloquinone) (Friedrich, 1988).

1.2 Proteins

Proteins are large biomolecules which constitute for more than 50% of the dry weight of the cell (McMurry, 1990; Campell, 1996). They perform very important functions in human body such as transporting, metabolic control, catalysis of chemical transformation and structural (Delvin, 1997).

1.2.1 Protein structure

1.2.1.1 Amino acids and peptide bonds

A human has many thousands of proteins; all of them are polymers of only 20 amino acids which are the building blocks of proteins while each protein has its specific function (Campell, 1996; McMurry, 1990). Amino acids are organic molecules which consist of an amino group (NH_2), a carboxyl group ($\acute{C}OOH$), a hydrogen atom, and a side chain (R-group) which differ from one amino acid to the other; all of these groups are covalently attached to a central carbon atom (C_α) as shown in (Fig.1.4) (Grooper, et al., 2009; Murry, 1990; Campell, 1996).
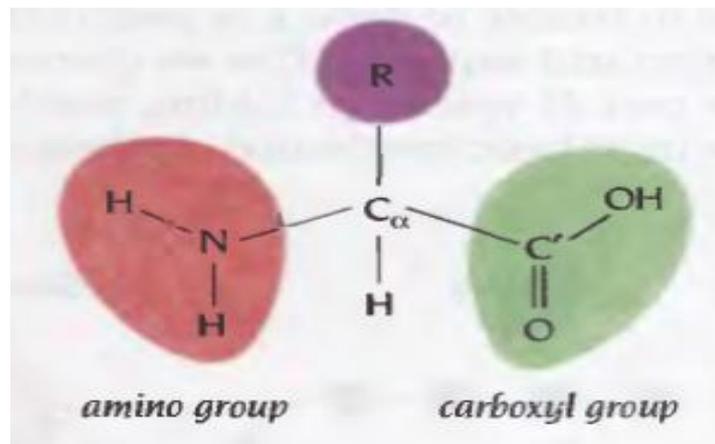
Fig 1.4: Schematic diagram of an amino acid (Branden, et al., 1999).

The side chain may be the hydrogen atom or a carbon skeleton, it contains atoms that can be polar (hydrophilic), nonpolar (hydrophobic) or charged, so that the physical and chemical properties of the side chains determine the amino acid characteristics (Branden, et al., 1999; Campell, 1996).

Amino acids are linked to each other by forming a peptide bond (also called amide bond) between the nitrogen atom in the amino group of one amino acid and the carbon atom in the carboxyl group of the following one as in (Fig.1.5).
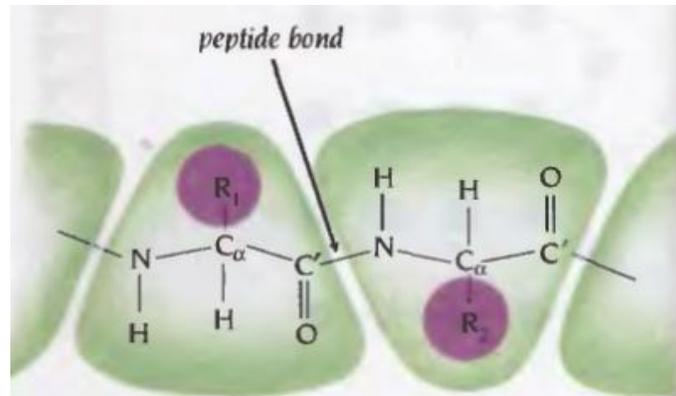
Fig 1.5: Peptide bond between amino acids (Branden, et al., 1999).

A protein consists of one or more Polypeptides which are chains with less than 50 amino acids (Campell, 1996; McMurry, 1990).

1.2.1.2 Structural levels of protein:

Proteins have four structural levels which determine their functions; these structures are primary, secondary, tertiary and quaternary structures.

Primary structure:
Is the sequence of amino acids, which is unique for each protein as shown in (Fig.1.6) (Grooper, et al., 2009).
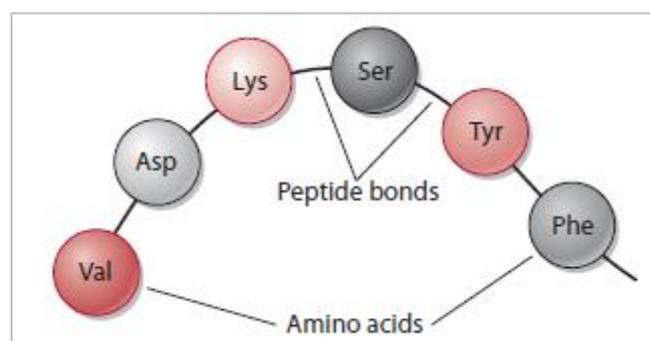
Fig.1.6: Primary structure of the protein (Grooper, et al., 2009).

Secondary structure:

Water-soluble globular proteins are folded by packing their hydrophobic side chains into the interior of the molecule; this makes the core of this protein hydrophobic where the surface of it is hydrophilic. Packing the hydrophobic side chains into the interior of the molecules needs the folding of the main chain which is highly polar (i.e., hydrophilic), this polar- main chain is neutralized in hydrophobic environments inside the protein by forming hydrogen bonds, which are a weak electrical attraction between the hydrogen atom and negatively charged atom such as nitrogen (Branden, et al., 1999; Grooper, et al., 2009).

These folding forms the secondary structure of the protein, there are many types of secondary structure according to the way of folding which are α- helices, β - sheets, β - turns and unordered structures (Grooper, et al., 2009).

α- helices are formed when a polypeptide chain coiled on itself by forming a hydrogen bonds between the $\acute{C} = O$ of n amino acid and NH of n + 4 amino acid, and a cylindrical shape is resulted as shown in (Fig.1.7) (Branden, et al., 1999; Grooper, et al., 2009).
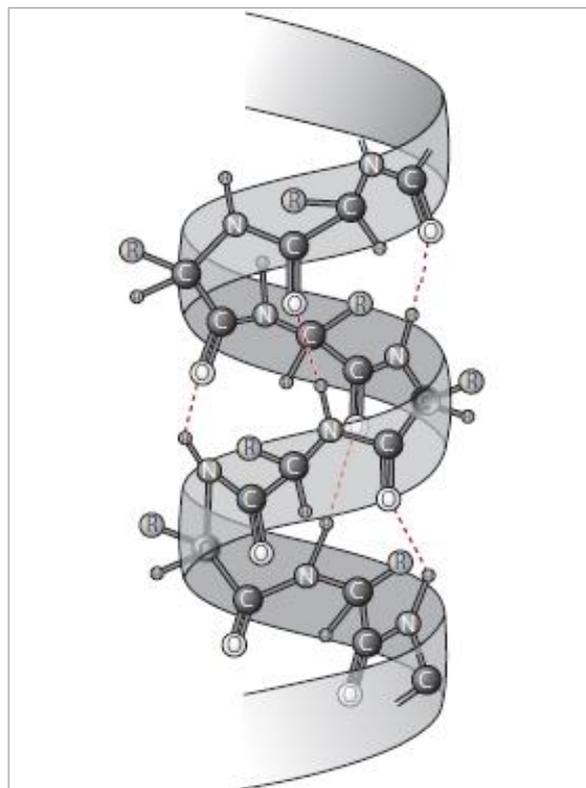
Fig 1.7: α- helix. (Grooper, et al., 2009)

All of the NH and $\acute{C} = $ O are joined by hydrogen bonds except the first NH and the last $\acute{C} =$ O groups making the ends of the- helix polar and always at the surface of the protein molecule.

All the hydrogen bonds in α- helix point in the same direction which is parallel to the helical axis, and the polarity of the main chain make a dipole moment which also points parallel to the helical axis forming a partial positive and negative charges at NH and $\acute{C} = $ O ends respectively of the α- helix. Charged ligands will be attracted to the group of different sign and bind with it (Branden, et al., 1999).

β – sheets: in contrast to the α- helix which is formed from one continues region, it is a combination of several regions of the polypeptide chain. It consists of two β – strands lying side by side and connected by hydrogen bonds between the two strands – backbones as shown in (Fig.1.8). The resulted β – sheet is called the pleated sheet (Campell, et al., 2008).
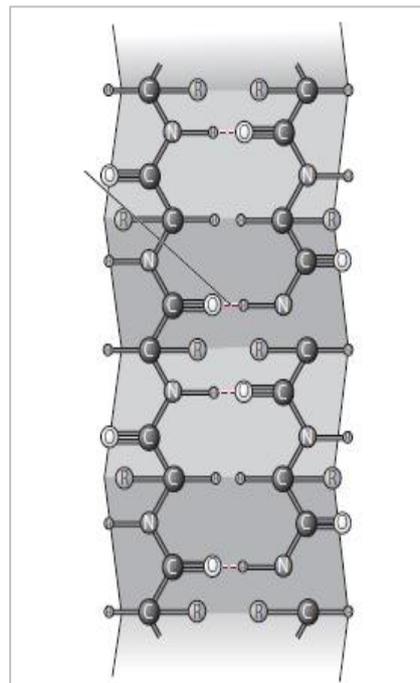
Fig 1.8: β – pleated sheet (Grooper, et al., 2009).

There are two ways for forming a pleated sheet; in the first way all the amino acids on the β strands points in the same directions, NH group on the first strand faced to the $\acute{C} = $ O group of the second strand of the sheet; such sheet is called parallel β – pleated sheet, where in

antiparallel β – pleated sheet the NH group of the first strand facing $\acute{C} = O$ group of the second strand followed by $\acute{C} = O$ group facing the NH group as shown in (Fig.1.9).
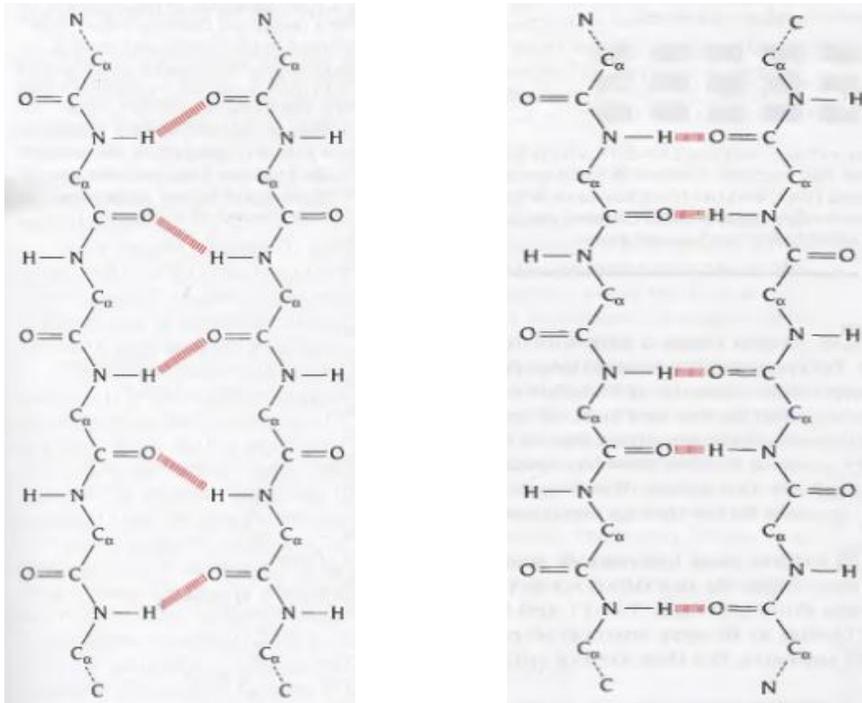
Fig 1.9: (a): Parallel β – pleated sheet, (b): antiparallel β – pleated sheet (Branden, et al., 1999).

Unordered structures: are loops that connect between different α – helices and β – sheets as shown in (Fig.1.10), these loops are at the surface of the molecule and exposed to the solvent. The main chain of these loops don't form hydrogen bonds between its amino acids, this help it to form hydrogen bonds with water molecules, and its side chains are polar, enabling several molecules to bind to it.
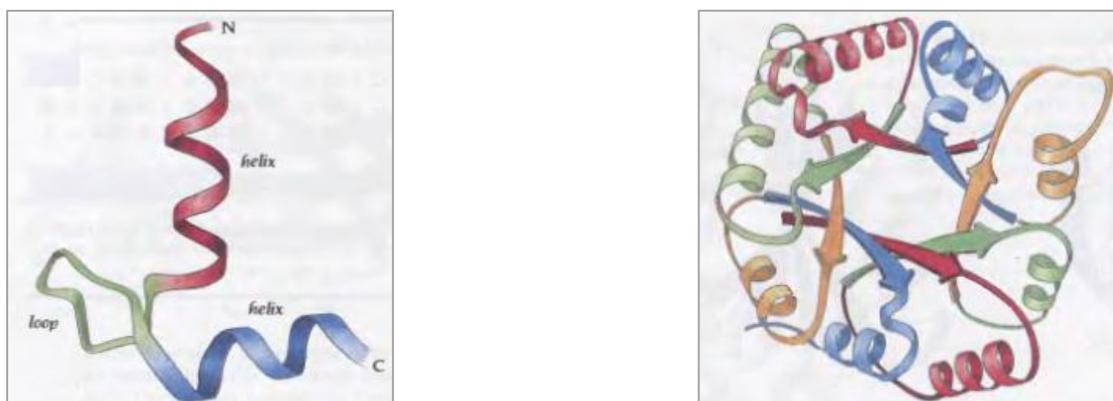
Fig 1.10: β – loops (Branden, ert al., 1999).

β – turns: are loops that connect the adjacent strands in antiparallel β – pleated sheet as shown in (Fig.1.11) (Branden, et al., 1999).
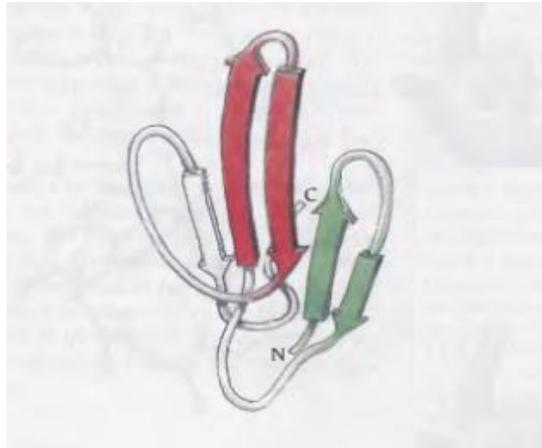
Fig 1.11: β – turns (Branden, et al., 1999).

Tertiary structure: the three- dimensional space resulted from the different secondary structure elements through the interactions between the side chains; these interactions can produce a linear or spherical structure

Quaternary structure: is the overall protein resulted from the interactions between the different polypeptide chains (Campell, 1996).

1.2.2 Human Serum Albumin (HSA)

HSA is the major protein component of blood plasma (approximately 60 % of the total protein) (Stan, et al, 2009) with a high concentration of 40 mg/ml (N'soukpoe-Kossi, et al., 2006; Ouameur, et al., 2004). It consist of 585 amino acids which contains 17 disulfide bridges, one free thiol (Cys 34) and a single Tryptophan (Trp 214) (He, et al., 1992) HSA is a globular protein, and contains three structurally similar domains (I, II, and III) as shown in (Fig. 1.12) (Barth, et al., 2009)
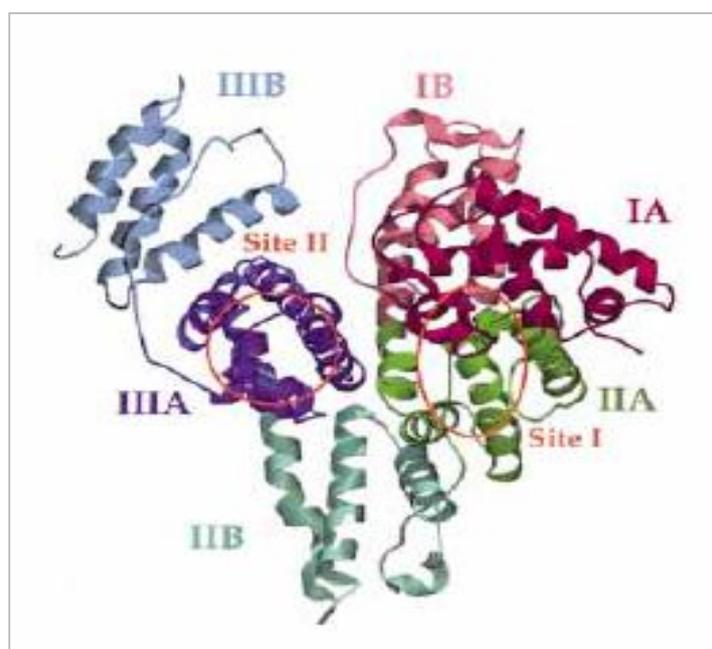
Fig 1.12: Domains (I, II, and III) in HSA (Kragh-Hansen, et al., 2002).

Each domain is divided into two subdomains, A and B. Most drugs have specific binding sites which are none as Sudlow's site I and site II, and locate in sub domains IIA and IIIA respectively (Tavirani, et al., 2005), whereas aromatic and heterocyclic ligands were found to bind within two hydrophopic pockets in sites I and II (Tajmir-Riahi, 2006).

Due to multiple binding sites, HSA serves as a major plasma carrier for a wide variety of endogenous and exogenous compound (Karnaukhova, 2007). In addition to its function in transporting materials due to its high affinity to bind ligands, it is also responsible for the maintenance of blood pH, the drug disposition and efficiency, and the contribution of colloid osmotic blood pressure (Wang, et al., 2008).

1.3 Motivation

Spectroscopic study for the interaction between Vitamin B_{12}, Vitamin A and HSA were carried out and published in (Hou, et al., 2008).Whereas, interaction between Vitamin k and HSA was not studied. In this thesis, the interaction of HSA with Vitamin $K_1$is studied using FTIR absorption spectroscopy and UV-VIS absorption spectrophotometry.

This thesis contains five chapters; the first chapter is an introduction, where the second chapter contains theoretical background from that the reader continues to the experimental part and understand data analyzing. In chapter three, the experimental part including samples preparations and equipment are described in details. Chapter four describes the results obtained and data analyzing. The final chapter contains the conclusion and the future work.

Chapter Two

Instruments and theoretical background

Chapter two

Instruments used and theoretical background

2.1 Instruments used:

The following spectrometers were used to maintain a spectrum for each sample from which we obtain the information about the interaction between HSA and Vitamin K_1.

2.1.1 FTIR spectrometer:

For FT-IR measurements, A Bruker IFS 66/S spectrometer which is shown in (Fig.2.1.a) was used in the mid-infrared spectral range of (4000 – 400) cm^{-1}.
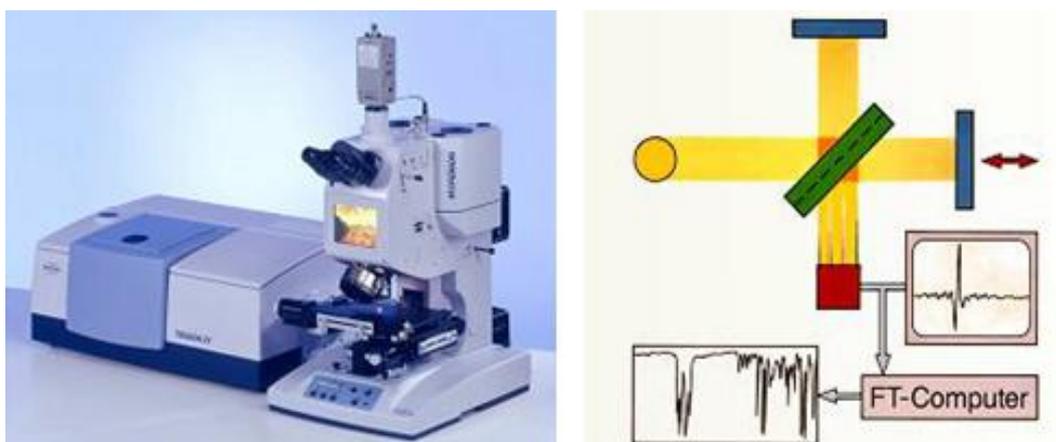
Fi g 2.1: (a): Bruker IFS 66/S spectrometer, (b): Michelson interferometer (OPUS

Bruker manual, 2004).

This spectrometer consists of several different modules, which are described in (Table.2.1).

Table 2.1: Bruker IFS 66/S spectrometer models and their descriptions (IFS 66v/S user's manual, 1998).

Module	Contents/ Description
Optical Bench	Interferometer, optics, detector, sample chamber, vacuum valves
Electronics Unit	Control electronics (source, optics, etc.), power supplies
Source Cooling System	Thermostatically controlled closed loop water circulator for sources
External Vacuum System	Pump, demister, bellows and pipes and valves to pump and backfill the optical bench.

The interferometer which is represented in (Fig.2.1.b) is a Michelson interferometer which was described previously in (Sec.2.8.2.1) with a KBr beam splitter. And the aperture which was used is 8 mm; since we found that this aperture gives the best signal to noise ratio. The sample holder with a hole A (Fig.2.2) , where the beam must pass through the center of this hole, and the beam holder is aligned on a base plate.
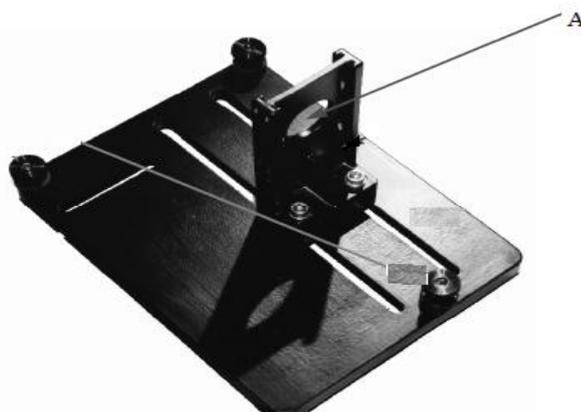
Fig 2.2: The sample holder and its base plate (IFS 66v/S user's manual, 1998).

The spectrometer was continuously purged with dry air during the measurements, Where a MCT detector was cooled using liquid nitrogen.

Table 2.2: Some of the optional detectors that can be used (IFS 66v/S user's manual, 1998).

Optional Detector	Operating Temperature
Si diode	Room
Ge diode	Room
InSb	Liquid N_2
FIR-DLATGS	Liquid N_2
MCT	Liquid N_2
InGaAs	Room

2.1.2 UV-VIS spectrophotometer:

A NanoDrop (ND – 1000) spectrophotometer which is shown in (Fig.2.3) was used to give the absorption spectrum in the range of (220 -750) nm. It has two fiber optic cables; the receiving and the source fibers with a gap between their ends. The light source is a pulsed xenon flash lamp, and a spectrometer utilizing a linear CCD array is used to analyze the light after passing through the sample. Special software run from a PC controlled the instrument, and the data is logged in an archive file on the PC.

Fig 2.3: NanoDrop (ND – 1000) spectrophotometer

2.2 Theoretical background

Spectroscopy is one of the corner stones of science. It can provide us with information about atoms and molecules; such as the strength of the bonds between atoms and the shapes of the molecules such as proteins and track changes in their structures.

This section contains eight subsections; the first five sections talk about the electromagnetic spectrum and the vibrational spectroscopy which we used to study the changes in the HSA secondary structure after interaction with Vitamin K_1. Those sections are about the absorption of infrared light, the vibrational energies for the molecules, the normal modes of vibrations and the group frequencies, the types of molecular vibrations, the Infrared (IR) spectrometers and the theory and advantages of FTIR spectrometers and finally the interpretation of IR- spectra. The sixth section is about the UV-VIS spectroscopy which we used to find the value of the binding constant between the HSA and the vitamin, where the seventh section is about the proteins and their structures and the final section describes the domains in HSA to which ligands bind.

2.2.1 Electromagnetic spectrum and absorption of light

Electromagnetic radiation consists of alternating electric and magnetic fields (Larkin, 2011), these fields propagating with speed of light as sine waves oscillating in phase in single planes which are at right angles to each other (Stuart, 2004). So it can be considered as plane- polarized radiation (Michael Hollas, 2004). The directions of the electric and magnetic field vectors represented by E and B respectively are shown in (Fig.2.4) (Stuart, 2004; Michael Hollas, 2002).
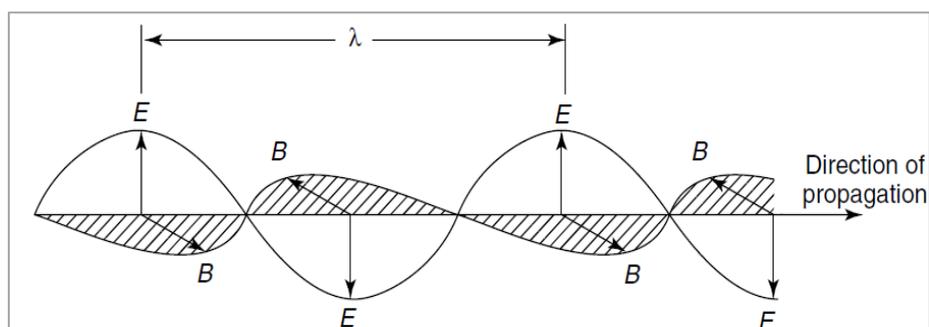
Fig 2.4: Representation of an electromagnetic wave (Stuart, 2004).

Electromagnetic spectrum is a broad spectrum of continuous energy, it can be divided into different regions as shown in (Fig.2.5) according to their energies and hence their chemical and physical effects they can produce on matter during interaction with it (Stuart, 2004; Derrick, et al, 1999), for example; Microwave radiation can change the rotational energy of molecules, Visible and Ultraviolet Visible radiations changes the electronic energy of the atoms and molecules and the absorption of IR radiation causes changes in the vibrational energies of molecules.
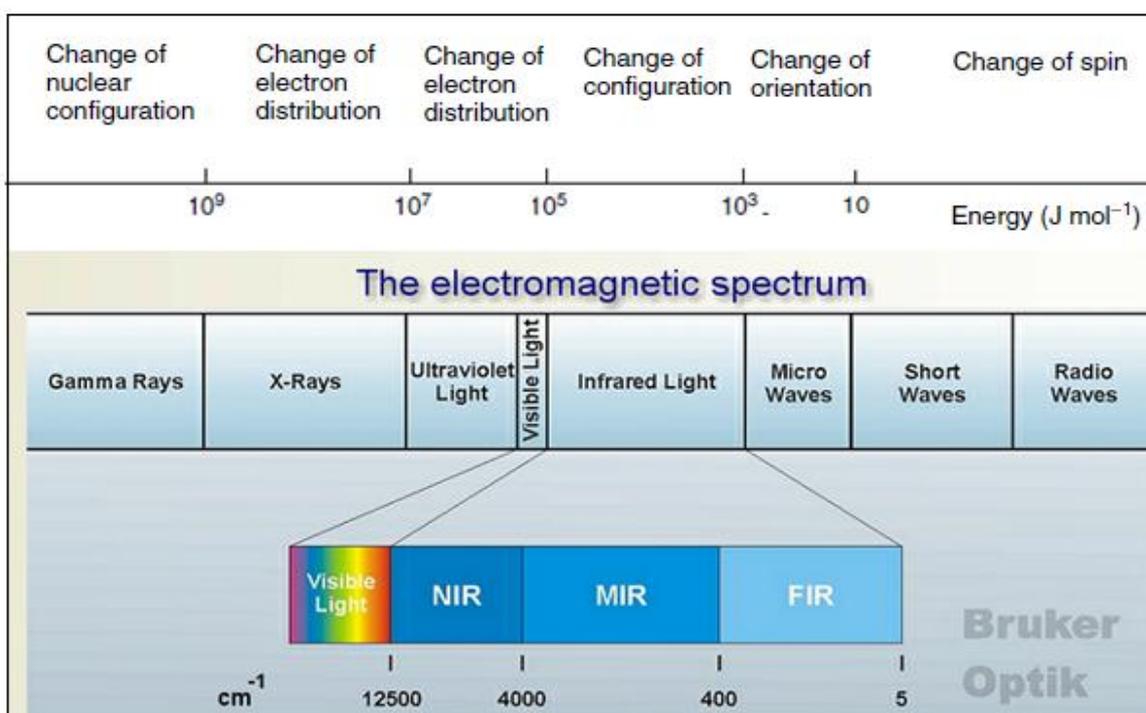
Fig 2.5: Regions of the Electromagnetic spectrum (OPUS Bruker manual, 2004; Stuart, 2004).

All energies of the electromagnetic spectrum can be considered as waves that move at the speed of light, while the types of radiation differing only in properties such as amplitude, frequency, and wavelength (Derrick, et al., 1999).

The amplitude is the height, or maximum size of the wave and corresponds to the intensity, the frequency v, which is the number of oscillations, or waves, per unit time-that is, cycles per second, the wavelength λ, which is the distance between two successive maxima or minima of a wave-that is, the length of one wave and the wavenumber $\tilde{v}$, which is the number of waves per unit length and can be expressed in cm^{-1} as:

$$\tilde{\nu} = \frac{1}{\lambda} \qquad (1)$$

The wavelength of the radiation is inversely proportional to frequency. Thus, high-frequency radiation has short wavelengths (Derrick, et al., 1999; Larkin, 2011).

In quantum theory, the source of electromagnetic radiation emits the radiation in discrete units of energy called photons where the photon frequency, ν, and its energy E_p, are related to each other by:

$$E_p = h\nu \qquad (2)$$

Where h is Planck's constant (6.6256× 10^{-27} erg sec) (Larkin, 2011).

When the light incident on the mater, a photon may be absorbed, scattered or may be transmitted through it without any interaction. If the energy of an incident photon equals to the energy gap between the ground and the excited states of a molecule, the photon may be absorbed and the molecule excited to the higher energy state with a change of its energy equals to E_p as shown in (Fig.2.6) (Ewen, et al., 2005).
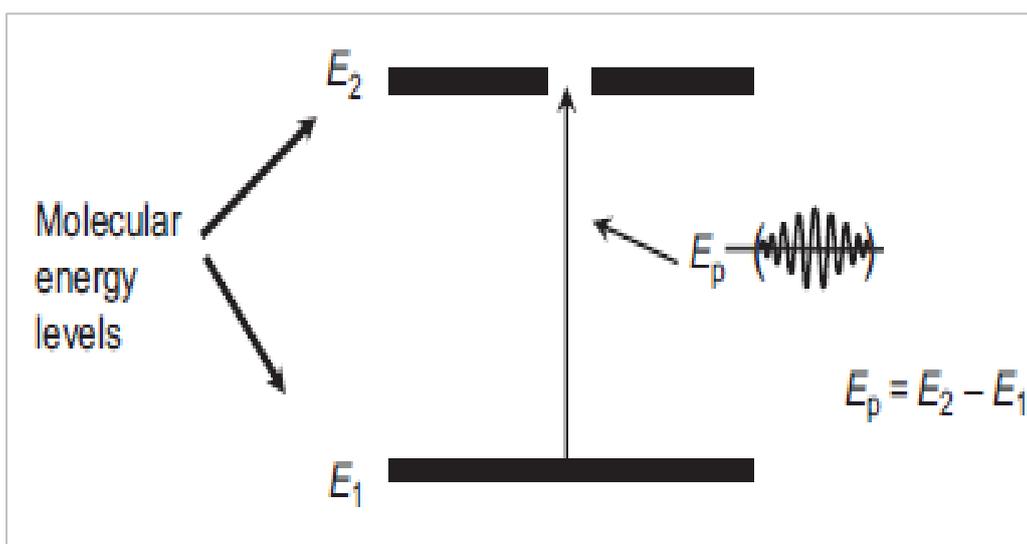
Fig 2.6: Absorption of electromagnetic radiation (Larkin, 2011).

The energy possessed by a molecule from electromagnetic wave at any given moment is given by:

$$E_{total} = E_{electronic} + E_{vibrational} + E_{rotational} + E_{translational} \qquad (3)$$

The translational energy ($E_{translational}$) describes the displacement of molecules from its equilibrium position. Where for rotational energy ($E_{rotational}$) which is the result of the absorption of energy within the microwave region, the molecule rotates around its center of mass.

The electronic energy ($E_{electronic}$) is due to the transitions of electrons as they are distributed throughout the molecule, either localized within specific bonds, or delocalized over structures, such as an aromatic ring.

The vibrational energy corresponds to the absorption of energy by a molecule for the atoms to vibrate about the mean center of their chemical bonds (i.e. they change their relative positions about the mean position to maintain a minimum energy by balancing the repulsive and attraction forces between the atoms and their constituents) (Coates, 2000; Banwell, 1972; Derrick, et al., 1999).

2.2.2 Vibrational energy

2.2.2.1 Vibrational energy for diatomic molecule:

In diatomic molecule, such as HCl and NO, bonds between the atoms can vibrate by two ways which are stretching or compression (Stuart, 2004; Larkin, 2011).

2.2.2.1.1 Harmonic oscillation:

The displacement of each atom in the molecule from its equilibrium position changes periodically with time with the same frequency but with different amplitudes. Thus the displacement of each atom as a function of time is plotted as a sinusoidal wave as in (Fig.2.4) (Larkin, 2011).

2.2.2.1.1.1 Classical approach:

We can imagine the atoms in a molecule connected by chemical bonds as balls of masses m_1 and m_2 connected by a massless string as in (Fig.2.7).
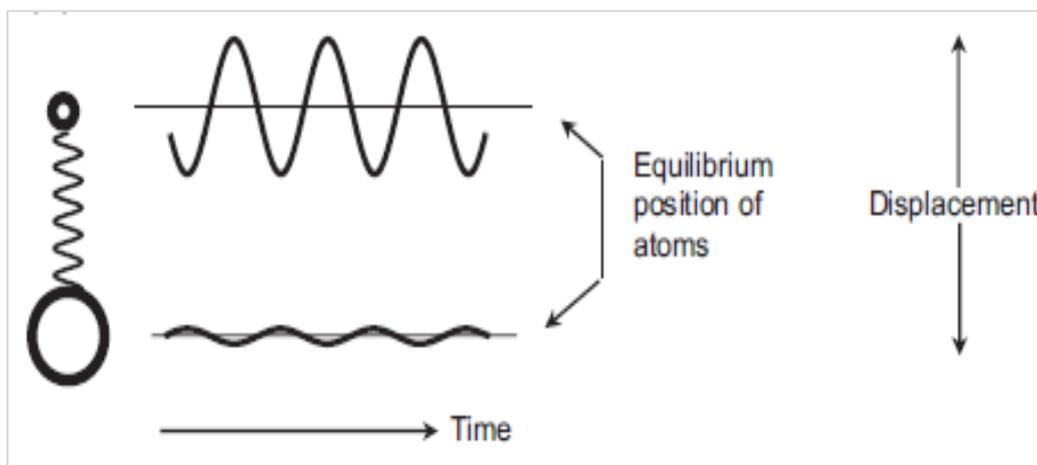
Fig 2.7: The ball and spring model for a diatomic molecule (Larkin, 2011).

This model is a harmonic oscillator for which the restoring force, **F**, of the spring is proportional to the displacement,**X,** of the atoms from their equilibrium position (Hooke's law).

$$\mathbf{F} = -\,\mathrm{k}\,\mathbf{x} \tag{4}$$

Where k is the force constant of the spring, and measures the strength of the bond between the two atoms.

Molecular bonds vibrate with a specific frequency that is called the vibrational frequency (ν).

$$\nu = \frac{1}{2\pi c}\sqrt{\frac{\kappa}{\mu}} \tag{5}$$

Where ν is the fundamental vibration frequency, c is the speed of light and μ is the reduced mass (Coates, 2000; Wartewig, 2003).

$$\mu = \frac{m_1 \, m_2}{m_1 + m_2} \tag{6}$$

And the vibrational energy is:

$$E = \frac{1}{2} K \, (r - r_{eq})^2 \tag{7}$$

Where r is the internuclear distance and r_{eq} is the equilibrium distance.

2.2.2.1.1.2 Quantum approach:

The quantum mechanical Hamiltonian for a one-dimensional harmonic oscillator is given by:

$$H = -\frac{\hbar^2}{2\mu} \frac{d^2}{dx^2} + \frac{1}{2} k \, x^2 \tag{8}$$

So, the Schrodinger equation is:

$$\frac{d^2 \psi_v}{dx^2} + \left(\frac{2\mu \, E_v}{\hbar^2} - \frac{\mu \, k \, x^2}{\hbar^2} \right) \psi_v = 0 \tag{9}$$

And the vibrational energy is given by:

$$E_v = h v \left(v + \frac{1}{2} \right) \qquad (v = 0, 1, 2,\ldots) \tag{10}$$

Where v: is the vibrational quantum number.

The only possible transitions are those which applies the selection rule $\Delta v = \pm 1$. The allowed vibrational energy levels for diatomic molecules are shown in (Fig.2.8) (Michael Hollas, 2004; OPUS Bruker manual, 2004; Gupta, 2001).
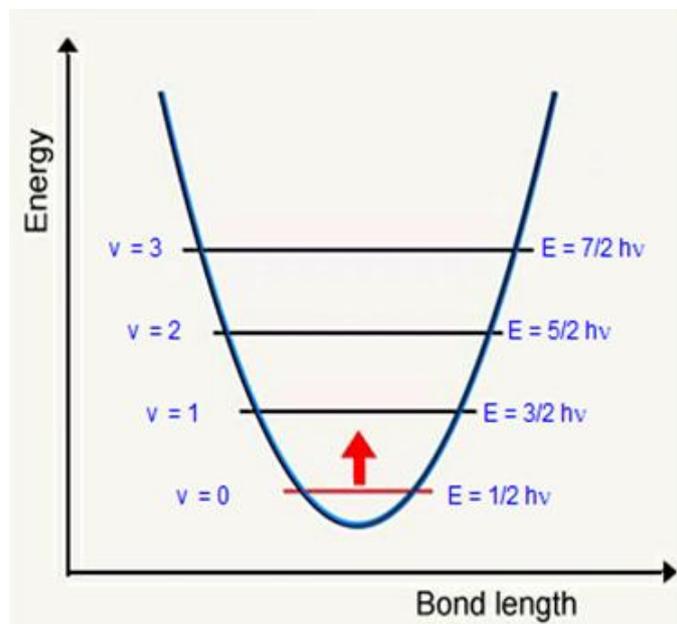
Fig 2.8: The allowed vibrational energy levels for harmonic oscillator (OPUS Bruker manual, 2004).

2.2.2.1.2 Anharmonic oscillation:

Real molecules don't obey the harmonic oscillations due to the following reasons; the first reason is that when two atoms approach each other, there must be a repulsive force between them, thus the vibrational energy will increase very rapidly.

The second reason is that when the two atoms go far away from each other, the bond between them will be broken; at this point, the vibrational energy equals the dissociation energy which is the point at which the molecule dissociates into its atoms. Thus the vibrational energy for diatomic molecule must be modified to apply the anharmonisity. The function which represens this is the Morse Function:

$$E = D_{eq} \left[1 - \exp\{a(r_{eq} - r)\}\right]^2 \tag{11}$$

Where D_{eq} is the dissociation energy, which is constant for a particular molecule.

When the Morse energy function inserted to the Schrodinger equation instead of (Eq. 5), then the vibrational energy will be:

$$\varepsilon_v = \left(v + \frac{1}{2}\right)\bar{\omega}_e - \left(v + \frac{1}{2}\right)^2 \bar{\omega}_e \chi_e \qquad (12)$$

Where $\bar{\omega}_e$, is the oscillation frequency expressed in wavenumbers and χ_e is the anharmonisity constant.

The selection rules are: $\Delta v = \pm 1, \pm 2, \pm 3$. Which are the same of that for the harmonic oscillator in addition to the possibility of larger jumps. The allowed vibrational energy levels for anharmonic oscillator are shown in (Fig.2.9).
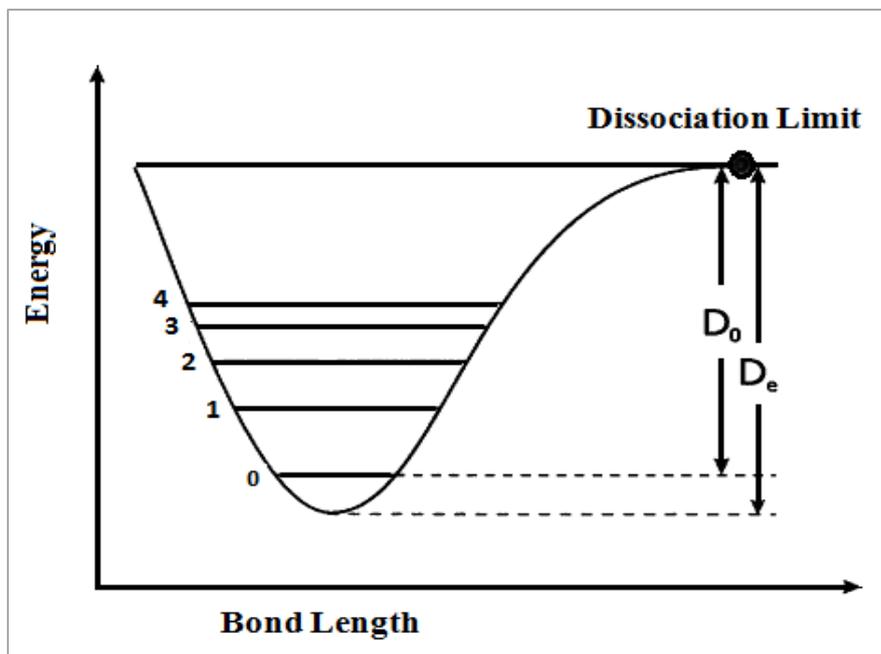
Fig 2.9: Potential energy curve for anharmonic oscillator (Bernath, 2005).

The transition from $v = 0$ to $v = 1$ is called the fundamental vibration, from $v = 0$ to $v = 2$ is called the first overtones and from $v = 0$ to $v = 3$ is called the second overtone. Where the transitions for $\Delta v = \pm 2, \pm 3$ are called the hot transitions, and these absorptions are weaker than the other transitions (Banwell, 1972; OPUS Bruker manual, 2004).

2.2.2.2 Vibrational energy for polyatomic molecules:

For polyatomic molecule there are 3N– 5 and 3N – 6 vibrational modes for linear and Non-linear molecules respectively as will be discussed in (Sec. 2.3.2). The vibrational energy for each normal mode is given by:

$$E_k = h\nu(\nu_k + \tfrac{1}{2})$$
(13)

Where ν_k is the vibrational quantum number of the Kth normal mode.

The total energy for Non-Linear molecule is the sum of the energies associated with each normal mode.

$$E_{vib} = \sum_{k=1}^{3N-6} \left(\nu_k + \frac{1}{2}\right) h\nu_k$$
(14)

The lowest vibrational energy (i.e. when $\nu_k = 0$), which is the energy of the ground vibrational level and called the zero-point energy, is given by:

$$E_\circ = \frac{1}{2} \sum_{k=1}^{3N-6} h\nu_k$$
(15)

When the anharmonicity is applied, then the vibrational energy for the polyatomic molecule is given by:

$$E_{vib} = \sum_{k=1}^{3N-6} \left(\nu_k + \frac{1}{2}\right) + \sum_{i=1}^{3N-6}\sum_{k\geq i} h x_{ik}(\nu_i + \frac{1}{2})\left(\nu_k + \frac{1}{2}\right) + h\,G_\circ$$
(16)

Where $G_\circ$ is a constant that arises partly from anharmonicity and partly from vibration-rotation interaction. It is usually omitted since it is very small, and it has been added to emphasize that the vibrational frequencies correspond to the equilibrium positions (Levine, 1975; Banwell, 1972).

26

2.2.3 IR spectroscopy:

Molecular spectroscopy is the study of the interaction between the electromagnetic radiation and matter (Banwell, 1972).

2.2.3.1 IR- absorption

When the energy of the incident light equals to the difference between two vibrational energy states, a photon of infrared light is absorbed making an increase in the amplitude of the bond vibrations and a transition from the lowest vibrational energy level to the higher one is resulted (Sathyanarayana, 2004; Pavia, 2001; Stuart, 2004).

In order for a photon of infrared light to be absorbed, there is another requirement rather than the energy matching, that is the electric field of the radiation must change the molecule's dipole moment as in (Fig.2.10) (Koenig, 1999; Sathyanarayana, 2004; larkin, 2011).
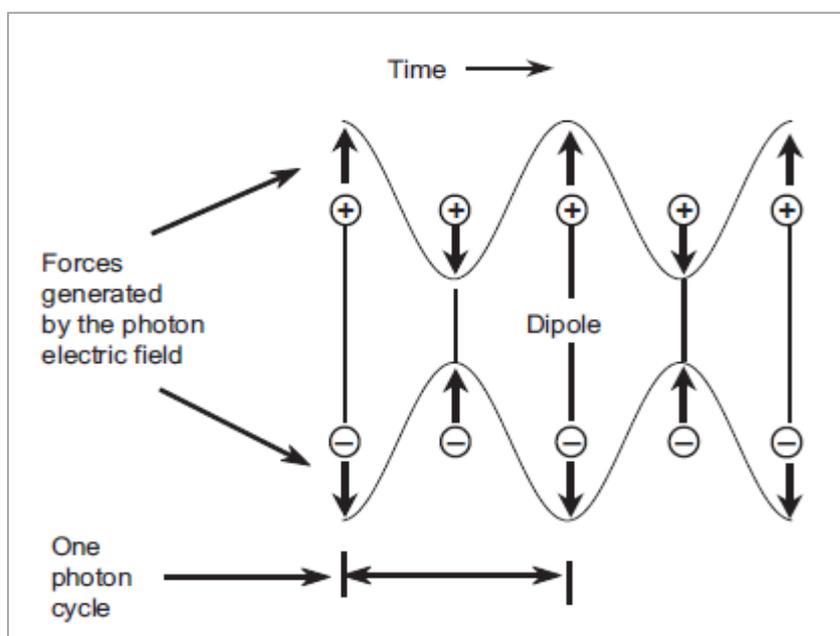
Fig 2.10: Changing of the molecule's dipole moment with the oscillating photon's electric field (larkin, 2011).

Homonuclear diatomic molecules such as H_2, N_2 and O_2 are IR- inactive molecules, since they have no dipole moment, where hetronuclear diatomic molecules such as HCl, NO and CO are IR- active molecules since they have dipole moments (larkin, 2011; Stuart, 2004).

2.2.3.2 Normal modes and degrees of freedom:

In a molecule, the atoms are constrained by molecular bonds to move together in certain specified ways, called degrees of freedom (Derrick, 1999). By considering that a molecule contains N atoms whose position can be referring by specifying three coordinates (e.g. the x, y and z Cartesian coordinates), so the total number of coordinates is 3N which is the total number of degrees of freedom for a molecule; three of them are due to translational movement and the other three in a nonlinear molecule are due to rotational movement, where in a linear molecule only two of them are due to rotational movement.

Normal mode of vibration is a molecular motion in which all the atoms undergo harmonic motion move in phase and with the same frequency (i.e. the frequency of normal vibration) but with different amplitudes. So for linear molecules, there are 3N− 5 vibrational mods, where for Non-linear molecules there are 3N − 6 vibrational mods as shown in (Table. 2.3) (Nikolić, 2011; Banwell, 1972; Michael Hollas, 2004; Steele, 1971; Svanberg, 2004).

Table 2.3: Degrees of freedom for polyatomic molecules (Stuart, 2004).

Type of degrees of freedom	Linear	Non linear
Translational	3	3
Rotational	2	3
Vibrational	3N - 5	3N - 6
Total	3N	3N

2.2.3.3 Molecular vibrations

Molecular bonds can vibrate mainly in different ways which are called modes of vibration; the first way in which the bond length is changed, is called the stretching vibration, where any other way is called the deformation mode such as bending vibration in which the bond angle is changed as in (Fig.2.11) (Stuart, 1997; Schrader, 1995; Sathyanarayana, 2004).
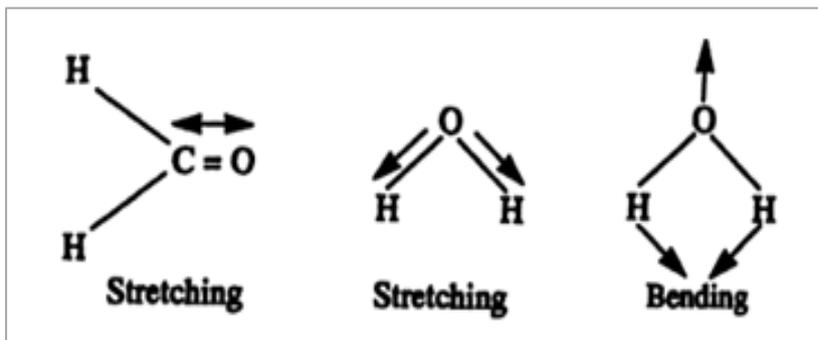
Fig 2.11: Stretching and bending vibrations (Stuart, 1997).

For a diatomic molecule there is only one normal mode which is the stretching vibration (Stuart, 2004), where polyatomic molecule, has stretching vibrations equal to the number of valence bonds in the molecule, and the remaining vibrations are bending vibrations (Sathyanarayana, 2004).

Molecular bonds may be stretch in-phase (symmetrical stretching) or out-of-phase (asymmetrical stretching) as in (Fig.2.12) (Stuart, 1997). Symmetrical molecules which are IR-active vibrate at fewer frequencies than that of the asymmetrical molecules (Stuart, 2004).
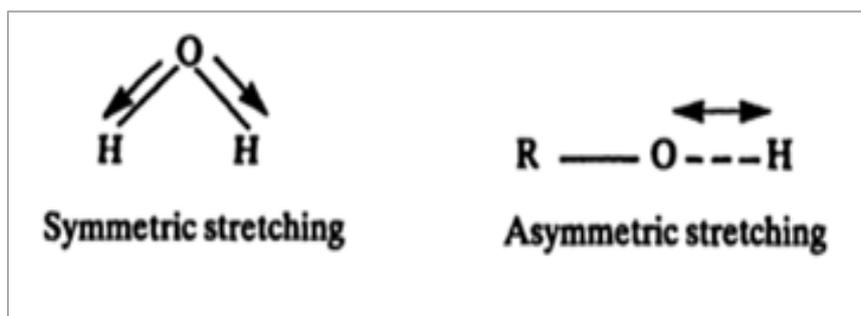
Fig 2.12: Symmetric and Asymmetric stretching vibrations (Stuart, 1997).

2.2.3.4 Group frequencies

Within the molecule there are two or more bonds which are close together and of similar energies (Ewen, et al, 2005), these bonds form a group which is called functional groups (such as a carbonyl group or an amide group), when the selection rules for IR absorption are Achieved, these groups absorbs a photon of IR light making the amplitude of the harmonic oscillation of the group's atoms larger than those of the other atoms in the molecule (Nakamoto, 1978; Derrick, 1999). A number of group vibration wavenumbers for some-stretching and bending vibrations are listed in (Table.2.4) (Michael Hollas, 2004).

This absorption occurs regardless of the rest of the molecule to which the functional group is attached; the frequency at which absorption occurs is called the group frequency and characteristic for that group (Derrick, 1999).

Table 2.4: Group vibration wavenumbers for some-stretching bending vibrations (Michael Hollas,2004).

Bond-stretching		Bond-stretching		Angle-bending	
Group	ω/cm^{-1}	Group	ω/cm^{-1}	Group	ω/cm^{-1}
≡C—H	3300	—C≡N	2100	≡C—H	700
=C(H)	3020	>C—F	1100	=C(H,H)	1100
except:		>C—Cl	650	—C(H,H,H)	1000
O=C(H)	2800				
>C—H	2960	>C—Br	560	>C(H,H)	1450
—C≡C—	2050	>C—I	500	C≡C—C	300
>C=C<	1650	—O—H	3600[a]		
>C—C<	900	>N—H	3350		
≡Si—Si≡	430	>P=O	1295		
>C=O	1700	>S=O	1310		

30

2.2.4 IR- spectra interpretation

When we plot the intensity of IR radiation absorbed or transmitted by the molecule versus the wavenumber we attain IR spectrum. The Y- axis may represent the absorbance or the transmittance of IR energy, where the x- axis represents the vibrational wavenumbers (Smith, 1996).

We can calculate the transmittance (T) from the absorbance (A) and vice versa according to the following relation:

$$A (\tilde{v}) = \log_{10} \frac{1}{T(\tilde{v})} \qquad \text{and} \qquad T(\tilde{v}) = \frac{I(\tilde{v})}{I_{\circ}(\tilde{v})} \qquad (17)$$

Where $I(\tilde{v})$ is the intensity of the transmitted IR energy and $I_{\circ}(\tilde{v})$ is the intensity of irradiating IR energy (Ohannesian, 2002; Griffiths ,2007).

IR spectrum provides us with quantitative or qualitative information.

2.2.4.1 Qualitative analysis

It provides us with qualitative information because each functional group in the molecule has its own peak of absorbance at specified frequency, so in our spectrum, if we have a peak at this frequency, it is evident that the molecule contain this functional group. For example, the peak around 3000 cm^{-1} points to that this molecule contains C-H bond stretching (Smith, 1996).

2.2.4.2 Quantitative analysis

It provides us with quantitative information because we can calculate the concentration of matter we deal with using Beer's Law, which relates the concentration to the absorbance at each component if the sample is a mixture as the following

$$A_i (\tilde{v}) = a_i(\tilde{v})b\ c_i \qquad (18)$$

Where $a_i(\tilde{v})$ is the linear absorption coefficient (cm^{-1}) at $\tilde{v}$, b is the thickness of the sample and c_i is the concentration at component i.

For N-component mixtures where more than one component absorbs at $\tilde{v}$, the total absorbance is given by: (Griffiths ,2007)

$$A(\tilde{v}) = \sum_{i=1}^{N} [a_i(\tilde{v}) \, b \, c_i] \qquad (19)$$

2.2.5 IR spectrometers:

There are many types of spectrometers that can detect the interaction between the IR-radiation and matter.

2.2.5.1 Dispersive spectrometers:

Prisms are the first dispersive infrared instruments, their popularity fell away in the 1960 s when the grating are manufactured due to their good quality (Stuart, 2004). Prisms and gratin are time consuming and less sensitive than other instruments because the different components of light (λ) are allowed to the sample separately. A schematic diagram of dispersive infrared spectrometers is shown in (Fig.2.13) (Pavia, et al., 2001).

A beam of IR radiation is produced by IR source, and then using mirrors this beam is divided into two parallel beams of equal intensities. The sample is placed in the way of one beam, and the other beam is used as a reference. The two beams then pass through a monochromator which disperse each into a continuous spectrum of frequencies of IR light. The monochromator consists of a beam chapper which is a rotating sector from which the two beams passes alternately to a diffraction grating (a prism in the older instruments).
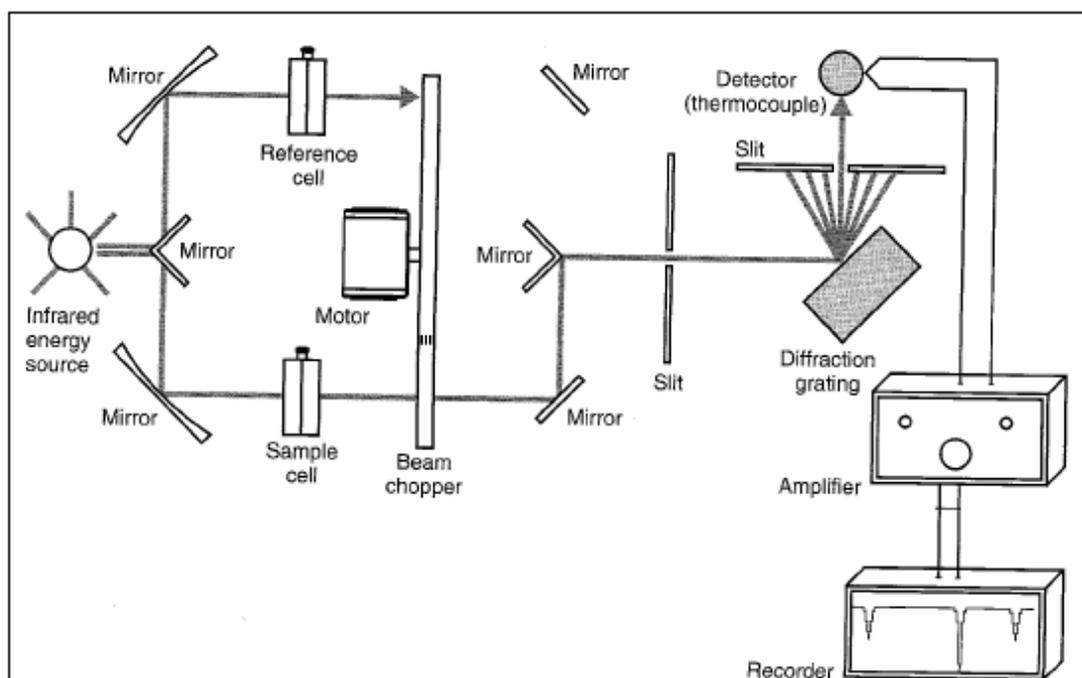
Fig 2.13: Schematic diagram of dispersive infrared spectrometers (Pavia, et al., 2001).

Then the diffracted beams are detected using a thermocouple detector. Diffraction grating rotates slowly, so it varies the frequency or the wavelength of radiation reaching the detector but in a long time (Pavia, et al., 2001; Stuart, 2004).

2.2.5.2 Fourier Transform Infrared (FTIR) Spectrometers:

The modern type which overcomes all the limitations of the older types is the (FTIR) spectrometers (Banwell, 1972).

2.2.5.2.1 Michelson interferometer

The heart of the FTIR spectrometer is a Michelson interferometer; which is a device that consists of an IR- source, two plane mirrors and a beam splitter. The layout of the Michelson interferometer is represented in (Fig.2.14) (Griffiths, 2007; Gregoriou, et al., 2006).
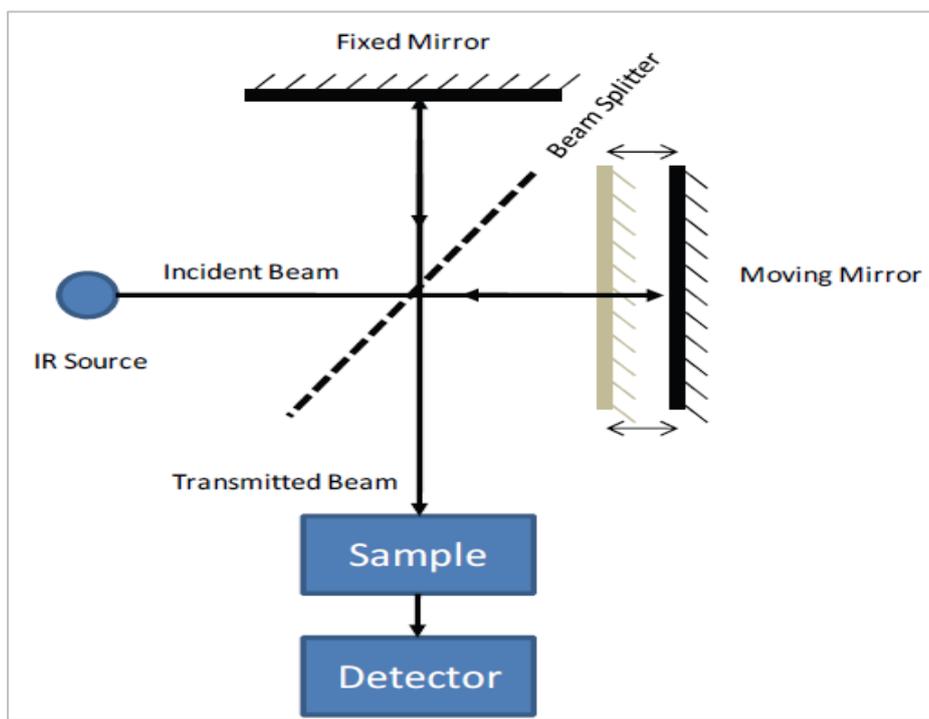
Fig 2.14: Schematic diagram of a Michelson interferometer (Nikolić, 2011).

The two plane mirrors are perpendicular to each other and bisected by a beam splitter which lies at a distance L from each one (Griffiths, 2007; OPUS Bruker manual, 2004).

One of the two mirrors is fixed and the other is movable to produce an optical path difference (δ) which equals twice of the distance that the mirror moving away from the beam splitter (Δ) (Smith, 1996).

$$\delta = 2\Delta \tag{20}$$

The incident beam of IR light is divided into two parts by a beam splitter which is a mirror placed to make an angle of $45°$ with the incoming radiation (Pavia, et al., 2001); it transmits only 50 % of the incident beam to the movable mirror and reflects the remaining part to the fixed mirror.

The reflected beam returns the fixed mirror after a distance L, and hence reaches the beam splitter after reflected from the fixed mirror after a path length of 2L. The transmitted beam returns the beam splitter after reflected from the movable mirror after a path length of (2L + δ) (OPUS Bruker manual, 2004). When the two beams returns to the beam splitter, they interfere constructively or destructively depending on δ (Griffiths, 2007; OPUS Bruker manual, 2004).

2.2.5.2.2 Interference of light:

The electric field strength E for a monochromatic wave with a wavelength λ is given by:

$$E = A\ e^{i(K.r - \omega t)} \tag{21}$$

Where A is the amplitude of the wave, r is the position vector, ω is the angular frequency, t is the time and K is the wave vector which can be expressed as:

$$k = |K| = \frac{2\pi}{\lambda} = 2\ \pi\ \tilde{v} \tag{22}$$

Where, both k and $\tilde{v}$ are called the wavenumber with the units (cm^{-1}) (Kauppinen, 2001). The intensity of the interference I of the electromagnetic wave, which is the power per unit area, is proportional to the square of its amplitude (Kauppinen, et al., 2001; siebert, et al., 2008).

When two electromagnetic waves:

$$E_1 = A_1 \, e^{i(k_x\,x - \omega t)} \quad \text{and} \quad E_2 = A_2 e^{i(k_x\,x - \omega t + \delta)} \tag{23}$$

Which have a phase difference δ, and propagating along the x- direction interfere with each other, their amplitudes are added and the resultant amplitude A as represented in (Fig.2.15) is: (Griffiths, 2007)

$$A = \sqrt{(A_1^2 + A_2^2 + 2A_1\,A_2 \cos \delta\,)} \tag{24}$$
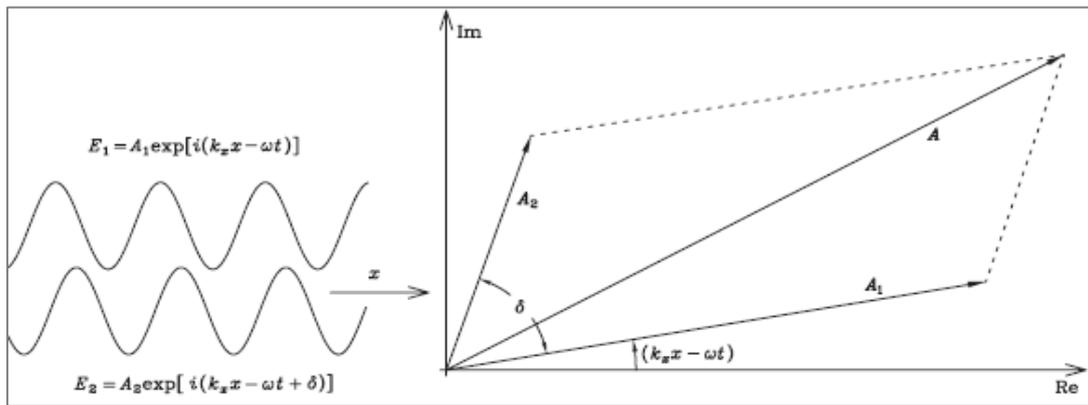
Fig.2.15: Interference of the two waves $E_1 = A_1 \, e^{i(k_x\,x - \omega t)}$ and $E_2 = A_2 e^{i(k_x\,x - \omega t + \delta)}$ A is the resultant amplitude (Kauppinen, et al., 2001).

In the case of the constructive interference, the interfering beams are in phase, and their amplitudes are added to give a more intense beam whose amplitude is greater than the amplitude of each of the individual beams (Smith, 1996).

The condition for the constructive interference is:

$$\delta = n\,\lambda \tag{25}$$

Where n is any integer with the values n = 0, 1, 2, 3,

When n = 0, the intensity of the beam resulted from the interference is maximum, and corresponds to the interference at zero path difference (ZPD) (OPUS Bruker manual, 2004; Smith, 1996).

In the case of destructive interference, the interfering beams are out of phase, and their amplitudes are added together and cancel each other, giving a beam of low intensity. The condition for the destructive interference is:

$$\delta = (n + \frac{1}{2}\ ) \lambda \qquad (26)$$

Where n is any integer with the values n = 0, 1, 2, 3, (Smith, 1996).

2.2.5.2.3 Intensity and theory of Fourier transformation:

The intensity of the beam resulted from the intensity of the interference I equals to the square of the resultant amplitude:

$$I = A^2 = A_1^2 +\ A_2^2 + 2A_1\ A_2 \cos \delta \qquad (27)$$

But the beam splitter divides the beam to two parts of equal intensity $I_{\circ}$, so:

$$I = 2\ I_{\circ} (1 + \cos \delta\ ) \qquad (28)$$

When the two beams have an optical path difference x, as in the interferometer, then the phase difference δ is given by:

$$\delta = \frac{2\ \pi x}{\lambda} = 2\pi\ \tilde{v}\ x \qquad (29)$$

Hence I is given by:

$$I = 2\ I_{\circ} (1 + \cos 2\pi\ \tilde{v}\ x\ ) \qquad (30)$$

Now, if the spectrum of the light source of intensity $I_\circ$ is continuous; that is consists of a wide band of wavenumbers then, the signal resulted from the interference from infinitesimal spectral between $\tilde{v}$ and $\tilde{v} + d\tilde{v}$ at a given optical path difference x is given by:

$$dF(x, \tilde{v}) = 2E(\tilde{v}) [1+\cos(2\pi \tilde{v} x)] d\tilde{v} \tag{40}$$

Where $E(\tilde{v})$ is the intensity of each of the two beams at a wavenumber $\tilde{v}$. So, the total signal from the whole spectral band is:

$$F(x) = 2 \int_0^\infty E(\tilde{v}) [1 + \cos(2\pi \tilde{v} x)] d\tilde{v} \tag{41}$$

Where, F(x) is called the interference record, which is the total reference of the whole spectral band.

Subtracting the constant term $\frac{1}{2}F(0) = 2\int_0^\infty E(\tilde{v}) d\tilde{v}$ from F(x), we have:

$$I(x) = F(x) - \frac{1}{2}F(0) = 2\int_0^\infty E(\tilde{v}) \cos(2\pi \tilde{v} x) d\tilde{v} \tag{42}$$

Where I(x) is called the interferogram, which is the plot of light intensity versus optical path difference as represented in (Fig.2.16).
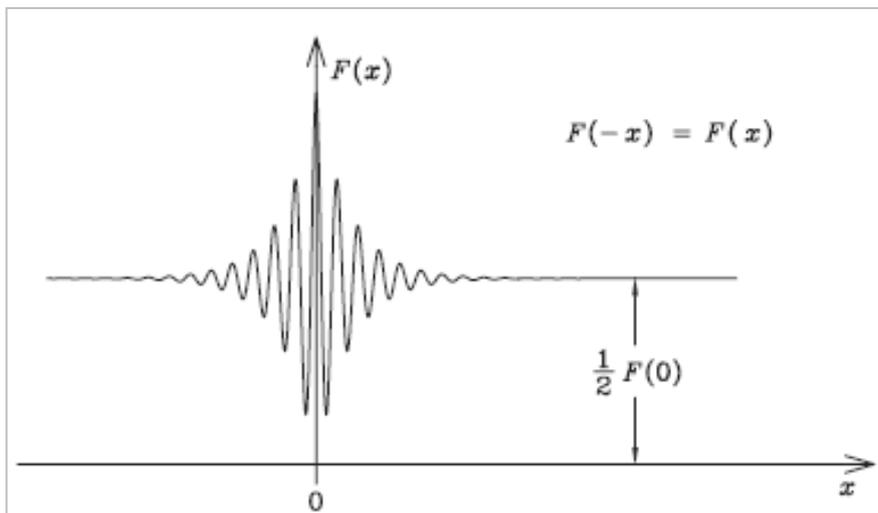
Fig.2.16: An interference record F(x) (Kauppinen, et al., 2001).

Mathematically, I(x) is the cosine Fourier transform of E($\tilde{\nu}$). So, the spectrum E($\tilde{\nu}$) is calculated from the interferogram by computing the cosine Fourier transform for I(x), as (Fig.2.17).
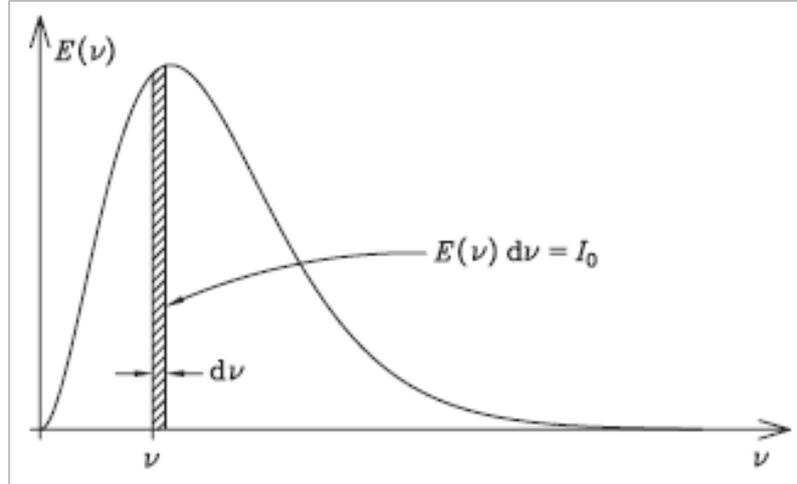
Fig 2.17: A wide-band continuous spectrum E($\tilde{\nu}$)and an infinitesimal monochromatic section of a width d$\tilde{\nu}$ (Kauppinen, et al., 2001).

E($\tilde{\nu}$) is an even function, that is E($\tilde{\nu}$) = E($-\tilde{\nu}$), so:

$$I(x) = \int_{-\infty}^{\infty} E(\tilde{\nu}) \cos(2\pi \tilde{\nu} x) \, d\tilde{\nu}$$
$$= \int_{-\infty}^{\infty} E(\tilde{\nu}) \, e^{i2\pi\tilde{\nu}x} \, d\tilde{\nu} = \mathcal{F} \{ E(\tilde{\nu}) \} \tag{43}$$

$$E(\tilde{\nu}) = \int_{-\infty}^{\infty} I(x) \cos(2\pi \tilde{\nu} x) \, dx$$
$$= \int_{-\infty}^{\infty} I(x) \, e^{i2\pi\tilde{\nu}x} \, dx = \mathcal{F} \{ I(x) \} \tag{44}$$

Where $\mathcal{F}$ is the Fourier transform (Kauppinen, et al., 2001; Griffiths, 2007). Noting that the spectrum of the source is 2E($\tilde{\nu}$), but for simplicity we avoided extra coefficients in front of the integral (Kauppinen, et al., 2001).

Equation.44 shows that we can measure the complete spectrum from 0 to $+\infty$ at infinitely high resolution. To achieve this, we would have to scan the moving mirror of the

interferometer to vary x from 0 to $+\infty$, which is experimentally impossible; the mirror retardation is limited, and hence the spectrum has a finite resolution (Griffiths, 2007).

The resolution for an FTIR instrument is limited by the maximum path difference between the two beams. The limiting resolution in wavenumbers (cm^{-1}) is the reciprocal of the path difference (cm), thus the maximum retardation for the interferometer is $\Delta = \frac{1}{\Delta\tilde{v}}$ (Stuart, 2004). Thus the spectrum resolution becomes limited by multiplying $E(\tilde{v})$ by a truncation function, D(x), which is unity between x = -Δ and + Δ, and zero at all other points.

$$D(x) = \begin{cases} 1 & if \quad -\Delta < x < \Delta \\ 0 & if \quad x > |\Delta| \end{cases} \tag{45}$$

Thus, entering $D(x)$ into (Eq. 43), yields that the truncated spectrum, G($\tilde{v}$) is given by:

$$G(\tilde{v}) = \int_{-\infty}^{\infty} D(x)\, I(x)\, \cos(2\pi\,\tilde{v}\,x)\ dx\ = \mathcal{F}\{(D(x)\,I(x)\,)\} \tag{46}$$

The Fourier transform (FT) of the product of the two functions is the convolution of the FT of each function.

$$G(\tilde{v}) = \mathcal{F}\{D(x)\} * \mathcal{F}\{I(x)\} = f(\tilde{v}) * E(\tilde{v}) \tag{47}$$

Where f ($\tilde{v}$) is given by:

$$f(\tilde{v}) = 2\Delta\,\frac{\sin(2\pi\tilde{v}\Delta)}{2\pi\tilde{v}\Delta} = 2\Delta\,\text{sinc}\,(2\pi\tilde{v}\Delta) \tag{48}$$

For a discrete source which emits light at wavenumbers $\tilde{\nu}_1$ and $\tilde{\nu}_2$, the measured is the resultant of the interferogram for each wave number, as shown in (Fig.2.18) (Griffiths, 2007).
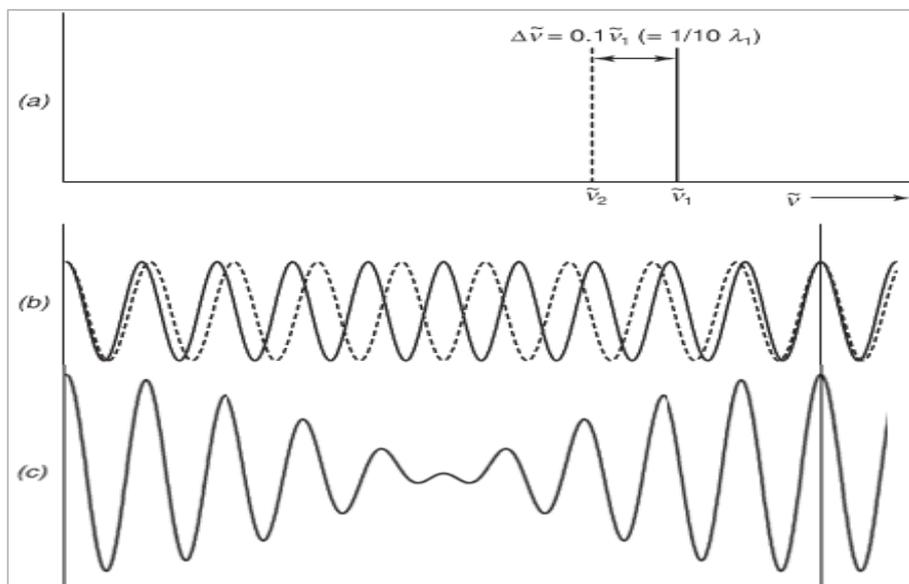
Fig 2.18: (a) Spectrum of the two lines of equal intensity at wavenumbers $\tilde{\nu}_1$ (soli line) and $\tilde{\nu}_2$(dashed line); (b) interferogram for each spectral line shown individually as solid and dashed line respectively; (c) the resulting interferogram (Griffiths, 2007).

For a continuous light source; that has a wide range of wavenumbers, the measured interferogram is the resultant of the interferograms that correspond to each wave number, which can be found by the integral of the interference patterns produced by each wavenumber (Griffiths, 2007; OPUS Bruker manual, 2004).

Nowadays, FTIR spectrometers have software which can display the absorption or transmission IR spectrums and manipulating them to enhance the required information (Smith, 1996).

2.2.6 UV- VIS spectroscopy:

When a radiation with wavelengths in the range of (190 to 800 nm), which is the range of the ultraviolet (UV) and Visible (VIS) region in the electromagnetic spectrum incidents on a molecule, the molecule will absorb the photon if its energy exactly equals to the energy difference between its excited and ground states (Pavia, et al., 2001). This absorption causes a transition of an electron from an orbital of a molecule in the ground state to an unoccupied orbital in the excited state (Valeur, 2001).

2.2.6.1 Molecular orbitals:

Molecular orbital (MO) is the space within which the electron forming the bond between the two atoms will spend 95% of its time (Banwell, 1972; Ohannesian, et al., 2002). MO originates from the overlapping of the atomic orbitals where the MO wave function ψ is a linear combination of the atomic wave functions χ_i.

$$\psi = \sum_i C_i \chi_i \tag{2.49}$$

Where C_i is the coefficient of the wave function χ_i (Michael Hollas, 2004).

For any overlapping, the molecular orbitals that can be formed are:

$$\psi_{MO} = \psi_1 + \psi_2 \qquad or \qquad \psi_{MO} = \psi_1 - \psi_2 \tag{2.50}$$

MO resulted from the constructive interference of ψ_1 and ψ_2 has a wave function ($\psi_{MO} = \psi_1 + \psi_2$) with an energy less than that for the individual atoms. This molecular orbital is called a bonding orbital. Whereas, the MO resulted from the destructive interference of ψ_1 and ψ_2 has a wave function ($\psi_{MO} = \psi_1 - \psi_2$) with an energy greater than that for the individual atoms. This molecular orbital is called an antibonding orbital (Banwell, 1972).

The way of the overlapping classifies the type of chemical bonding, and the occupancy of the molecular orbital is governed by the Pauli Exclusion Principle which says that the molecular orbital can contain no more than two electrons) (Ohannesian, et al., 2002).

A σ orbital can be formed either from two s atomic orbitals, or from one s and one π atomic orbital, or from two π atomic orbitals having a collinear axis of symmetry where the atomic orbitals overlapping along the line joining the nuclei of the bonded atoms. The bond formed in this way is called σ bond.

A π orbital is formed from two π atomic orbitals overlapping laterally. The resulting bond is called a π bond where the atomic orbitals overlapping at right angles to the line joining the nuclei of the bonded atoms. Because in σ bond the electronic charge is localized between two atoms, electronic repulsion prevents the formation of more than one σ bond between any two atoms in the molecule and the distribution of electronic charge in π bond is concentrated above and below the plane containing the σ- bond axis (Valeur, 2001; Ohannesian, et al., 2002).

A molecule may also possess non-bonding orbitals (n) orbitals that contain unshared pairs of electrons (Valeur, 2001; Pavia, et al., 2001). σ and π bonds and nonbonding electrons for formaldehyde molecule are shown in (Fig.2.19) (Valeur, 2001).
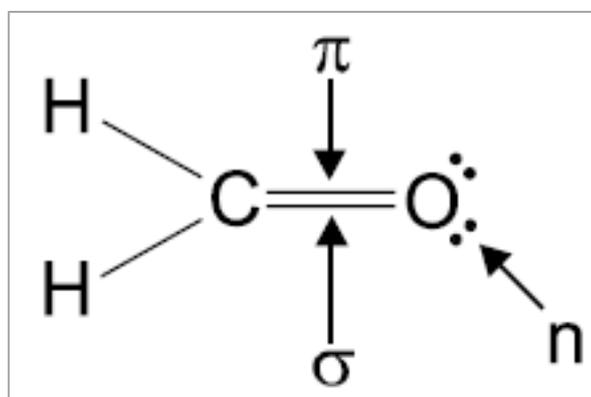
Fig.2.19: σ and π bonds and nonbonding electrons for formaldehyde molecule (Valeur, 2001).

2.2.6.2 Possible electronic transitions

The most probable transition is that from the highest occupied molecular orbital (HOMO) to the lowest unoccupied molecular orbital (LUMO) (Pavia, et al., 2001). Because there are several unoccupied orbitals which are the antibonding orbital with energy higher than that of the bonding and the n- orbitals, several electronic transitions are possible. The electronic molecular orbitals and the possible transitions between them are shown in (Fig.2.20) (Pavia, et al., 2001; Valeur, 2001).
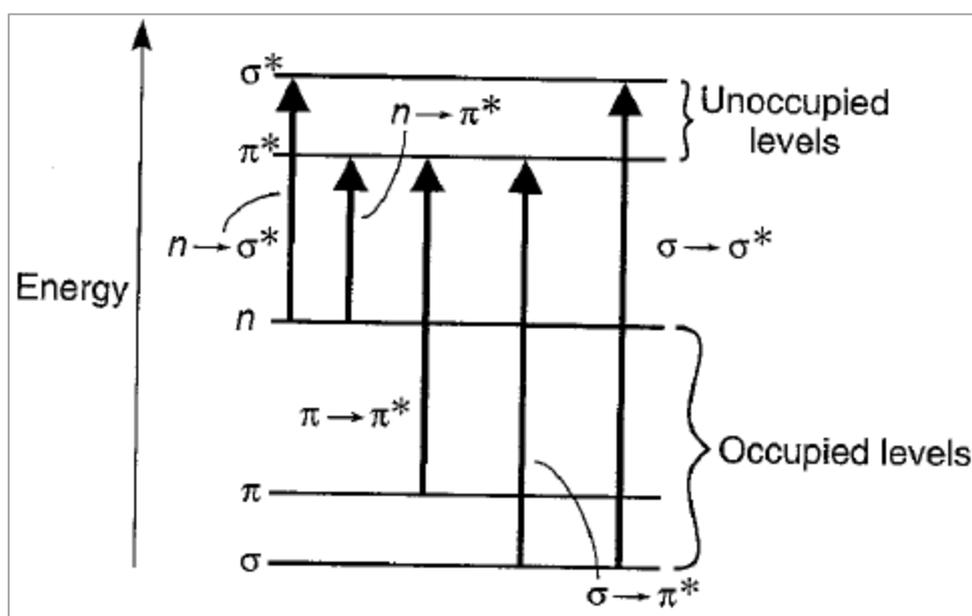
Fig.2.20: the electronic energy levels and the possible transitions between them (Pavia, et al., 2001).

The possible electronic transitions with their energies are generally in the following order: (Valeur, 2001).

$$n \rightarrow \pi^* < \pi \rightarrow \pi^* < n \rightarrow \sigma^* < \sigma \rightarrow \pi^* < \sigma \rightarrow \sigma^* \tag{51}$$

Chapter Three

Experimental Part

Chapter Three

Experimental Part

UV-VIS spectrometer (NanoDrop ND- 1000) and a Bruker IFS 66/s FTIR spectrometer are used to study the interaction between HSA and VitaminK$_1$ as the following sections describe.

3.1 Materials used and samples preparations:

3.1.1 Materials used:

HSA (fatty acid free), vitamin K_1 (Phylloquinone) are used without further purifications. Phosphate buffer Saline and ethanol were used to dissolve HSA and VitaminK$_1$. All of these samples were purchased from Sigma Aldrich Company.

Optical grade silicon windows (NICODOM Ltd) which were purchased from Sigma Aldrich Company were used as spectroscopic cell windows on which we prepare thin films of samples.

3.1.2 Samples preparations:

Solutions of HSA with different concentrations of Vitamin K$_1$ were prepared. Equal amounts of these solutions were spread on the silicon window and incubated at room temperature for 24 hours to form thin films.

3.1.2.1 Preparation of Phosphate buffer saline solution:

It was prepared by dissolving one foil pounch of Phosphate buffer saline in one liter of double distilled water.

3.1.2.2 Preparation of HSA stock solution:

An eighty mg of HSA with a molecular weight of 66.5 KDa was dissolved in 1 ml of (25 % ethanol in phosphate buffer of saline at a physiological pH 7.4) to get a final concentration of (40mg/ml) in the final HSA - VitaminK$_1$ solution.

3.1.2.3 Preparation of Vitamin K$_1$ stock solution:

Vitamin K$_1$ of molecular weight (450.7 g/mol) and density (0.984 g/ml) was dissolved in (25 % ethanol in phosphate buffer saline pH 7.4. Tthen the solution was placed in ultrasonic waterpath (SIBATA AU- 3T) for two weeks to ensure that all the amount of Vitamin K$_1$ was completely dissolved.

3.1.2.4 Preparation of HSA - Vitamin K$_1$ solutions:

The concentration of HSA was fixed at (40 mg/ml) in all samples. The concentration of Vitamin K$_1$ in the final HSA − Vitamin K$_1$ solutions was reduced such that the molecular ratios (HSA: VitaminK$_1$) are 1:20, 1:10, 1:5, 1:2 and 1:1 by mixing equal volume of HSA and Vitamin K$_1$.

3.1.2.5 Preparation of thin films:

50 μl of each sample of HSA–Vitamin K$_1$ solution was spread on a silicon window and incubated at room temperature for 24 hours to complete dryness and making thin films.

3.2 Experimental procedures:

3.2.1 UV-VIS measurement:

Measurements using UV-VIS spectroscopy is taken according to the following procedure:

Opening the sampling arm, 2µl of the sample is pipetted onto the lower measurement pedestal at the receiving fiber optic cable as in (Fig.3.1).

Fig 3.1: Measurement pedestal of Nano Drop (ND – 1000) spectrophotometer.

The sampling arm is closed, causing the liquid to bridge the gap between the fiber optic ends as in (Fig.3.2), and then a spectral measurement using the operating software on the PC is initiated.
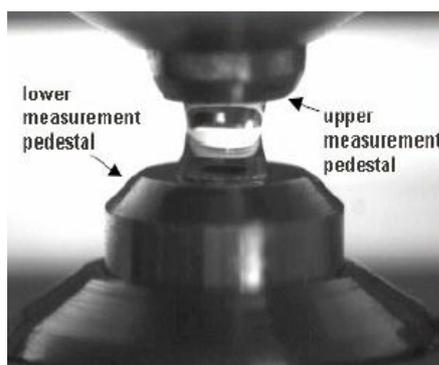
Fig 3.2: The gap between the fiber optic ends

The spectrophotometer is initiated using water, then a measurement for the solvent is taken, then the intensity transmitting through the solvent at each wave length in the range (220 - 750) nm is stored in the memory of the computer as a reference, which is called the blank.

After each measurement is finished, the upper and lower pedestals are cleaned using wipes to prevent carryover for samples differing in concentrations as in (Fig.3.3) .

Fig 3.3: Cleaning the instrument.

After that the spectrophotometer is planked, a measurement for each sample is taken, then the intensity of light that has transmitted through the sample is recorded, and the intensities for the blank and the samples are used to calculate the sample absorbance at each wavelength according to the following equation:

$$\text{Absorbance} = -\log(\frac{\text{Intensity}_{\text{sample}}}{\text{intensity}_{\text{blank}}}) \qquad (1)$$

After the measurement is finished, the data needed is logged in an archive file on the PC (NanoDrop (ND − 1000) spectrophotometer Version 2.5 User's Manual, 2006).

3.2.2 FTIR measurement:

3.2.2.1 Measurements using FTIR spectroscopy is taken according to the following procedure:

The electronic units of the Bruker IFS 66/S spectrometer is switched on choosing the range of the MIR that is $(4000 - 400)\ cm^{-1}$, and the liquid nitrogen compartment is filled with liquid nitrogen to cool the MCT detector. Using OPUS program which is on the computer, the spectral parameters is chosen such that: the spectral resolution is $4\ cm^{-1}$ and the average scan for each sample is 60 scans to increase the signal to noise ratio.

The sample holder holding the silicon window is placed inside the sample compartment and the interferogram signal is obtained for the clean silicon window as a reference and for each sample separately. Then, the program algorithm converts the interferogram to absorbance spectra using Fourier transformation.

3.2.2.2 Spectral manipulations and measurements:

The primary problem in IR spectral analysis of proteins is that the bands are a complex composite of overlapping component bands that represent different structural elements. (Pelton, 2000)

So, using manipulation menu bar, some spectral manipulation such as; smoothing, normalization, Baseline corrections, spectrum Fourier Self- Deconvolutin (FSD), curve fitting and second derivative resolutions where applied to increase the spectral resolution (Tajmir-Riahi, 2007).

These spectral manipulations in addition to peak picking and integration using evaluation bar, are used to study the secondary structure of the HSA protein and the changes on it after combined to the vitamin.

3.2.2.2.1 Smoothing

Smoothing is used to reduce the noise effect on the noisy spectrum, to enhance the data acquired from the spectrum (Smith, 1996). A smoothing function is basically a convolution between the spectrum and a vector whose points determined by the degree of smoothing applied. (Staurt, 2004)

3.2.2.2.2 Spectral Derivatives

The bottom of a downward pointing feature in a second derivative corresponds exactly to the wavenumber of maximum absorbance of a band in the original spectrum. If there is a region of a spectrum where several bands have overlapped to form one broad band, the number of downward pointing peaks in the second derivative gives a good estimate of the number of overlapped bands in the region (Smith, 1996).

3.2.2.2.3 Baseline correction

A baseline joining the points of lowest absorbance on a peak with reproducibility flat parts is used in quantitative spectroscopy; since the difference in the absorbance between the baseline and the top of the band then can be used (Staurt, 2004).

3.2.2.2.4 Fourier Self- Deconvolution

The purpose of the deconvolution is to mathematically narrow the width of the spectral bands (Griffiths, 2007). It is commonly performed on a region of the spectrum where several narrower bands overlap to give a broad band to determine the number and the peak positions of the overlapped bands (Smith, 1996).

3.3.2.2.5 Spectral subtraction

Spectral subtraction is performed when one desired to obtain the spectrum of a component in a mixture (Smith, 1996). If the interaction components results in a change in the spectral properties of either one or both of the components, the changes will be observe in the difference spectra (Staurt, 2004).

3.3.2.2.6 Curve-Fitting

Quantitative values of the band areas of the overlapped bands can be achieved using Curve-Fitting procedure which involves entering the values of the wavenumbers and width of the component bands (determined from the second derivative and deconvolution) (Staurt, 2004).

Chapter Four

Results and discussions

Chapter Four

Results and discussions:

Studying the interaction between HSA and Vitamin K_1 using UV-VIS absorption spectrophotometry and FTIR spectroscopy indicates that there is an interaction between the as the following sections describe.

4.1 UV-VIS absorption spectroscopy

The excitation has been done at 210 nm and the absorption occurred at 278 nm. The absorption spectrums for the samples of HSA with different molecular ratios of Vitamin K_1 are shown in (Fig.4.1).

It is clear that the absorption intensity increases with increasing the concentration of Vitamin K_1, where there are slight shifts in the peaks which indicates that there is an interaction between HSA and Vitamin K_1 and that the peptide strands of the protein extended more due to the addition of vitamin K_1 (Abu Teir, et al., 2012).

The result that confirm that there is an interaction between the HSA and Vitamin K_1 is that the free Vitamin K_1 has a little absorbance spectra, so the resulted absorption spectra is due to the interaction between the protein and the vitamin.
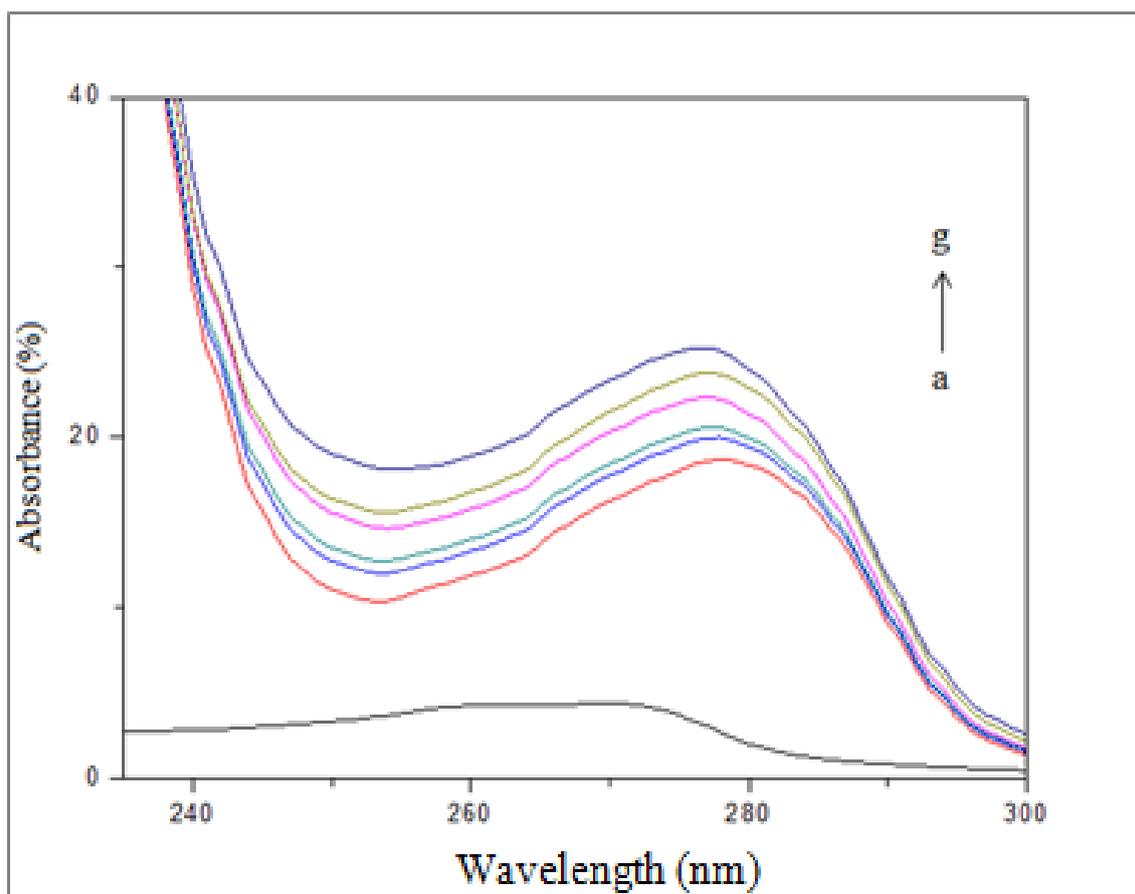
Fig 4.1: UV-VIS absorbance spectra of HSA with different concentrations of Vitamin K_1 (a=K_1 free, b=1:0, c=1:1, d=1:2, e=1:5, f=1:10, g=1:20)

4.1.1 Calculating the binding constant (K) between HSA and Vitamin K$_1$ using UV-VIS spectroscopy

The value of the binding constant (K) between HSA and Vitamin K$_1$ can be determined using the data obtained from the UV-VIS absorption spectrophotometry using a method described previously in many published articles (Abu Teir et al, 2012; Darwish, et al., 2010; Tajmir-Riahi, 2007). By assuming that there is only one type of interaction between HSA and Vitamin K$_1$ in the aqueous solution, we can form the following two equations:

$$\text{HSA} + \text{Vitamin K}_1 \quad \longleftrightarrow \quad \text{Vitamin K}_1\text{:HSA} \tag{1}$$
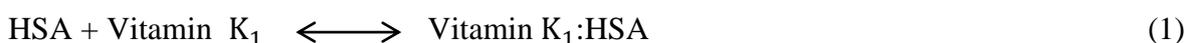
$$K = \frac{[\text{Vitamin K}_1 : \text{HSA}]}{[\text{Vitamin K}_1]\,[\text{HSA}]} \tag{2}$$

The value of the binding constant (K) can be calculated using the following equation (Abu Teir et al, 2012):

$$\frac{1}{A - A_\circ} = \frac{1}{A_\infty - A_\circ} + \frac{1}{K(A_\infty - A_\circ)} \times \frac{1}{L} \tag{3}$$

Where $A_\circ$ is the initial absorption of the free protein at 278 nm, A_∞ is the final absorption of the ligated protein, and A is the recorded absorption at different Vitamin K$_1$ concentrations (L) (Darwish, et al., 2010).

The double reciprocal plot of $1/(A - A_\circ)$ versus $1/L$ is linear as in (Fig. 4.2) and the binding constant (K) can be calculated from the ratio of the intercept to the slope can be found $60\ M^{-1}$. The value of the binding constant calculated show a weak HSA - Vitamin K$_1$ interaction by comparison to the other strong ligand–protein complexes with binding constants ranging from $10^5\ to\ 10^6\ M^{-1}$ (Ouameur et al., 2004). The reason for the low stability of the Vitamin K$_1$-HSA complexes can be attributed to the presence of mainly hydrogen bonding interaction between protein donor atoms and the Vitamin K$_1$ polar groups or an indirect Vitamin K$_1$-protein interaction through water molecules (Purcell, et al., 2000).
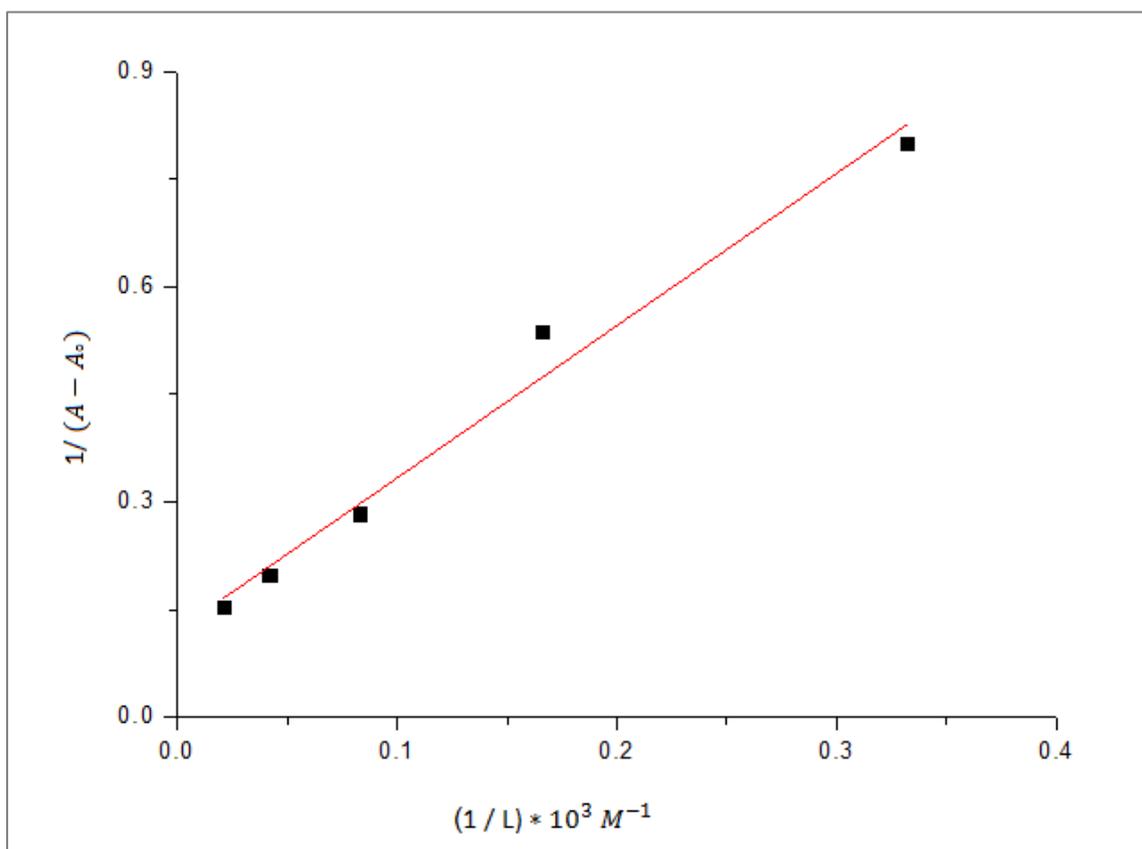
Figure 4.2: The plot of $1/(A - A_\circ)$ vs. $1/L$ for HSA with different concentrations of Vitamin K_1.

4.2 Changes in HSA secondary structure due to the interaction with Vitamin K_1 using FTIR spectroscopy

Mid- IR spectroscopy is one of the earliest techniques for studying the protein secondary structure (Luis, et al., 1999; Kong, et al., 2007; Byler, et al., 1986). FTIR spectroscopy can be used to determine the protein secondary structure in a wide range of environments (e.g., in solution as in the solid state) requiring less time and sample than other spectroscopic techniques need (Kong, et al., 2007; Jiang, et al., 2011). FTIR spectroscopy provides also information about the interaction between the protein and the ligand. (Fale, et al., 2011)

FTIR spectrum of a protein is composed of many vibrational bands arising from different functional groups such as N-H, C = O, and the amide groups. (Jiang, et al., 2011) So, IR spectra of proteins contain a number of the amide bands; the most popular ones in the ranges (1700-1600 cm^{-1}), (1600- 1480 cm^{-1}), (1330- 1220 cm^{-1}) are related to the bands which are called amides I, II and III respectively (Darwish, et al., 2010, Khan, et al., 2007).

Amide I band is primarily due to C = O stretching vibrations of the amide groups. (Byler, 1993) This band is the most widely used to study the protein; because it is more sensitive to the change in their secondary structure than other amide bands (Khan, et al., 2007, Fale, et al., 2011). Amide II band is primarily due to the N-H bending vibrations combined with C-N stretching vibration. (McLean, et al., 2000) where amide III region is due to the C-N stretching vibrations coupled with in plane N-H bending vibrations (Abu Teir et al, 2012), which are the same to that of amide II, albeit with a different sign in the combination of the coordinate as in (Fig. 4.3) (Siebert, et al,. 2008).
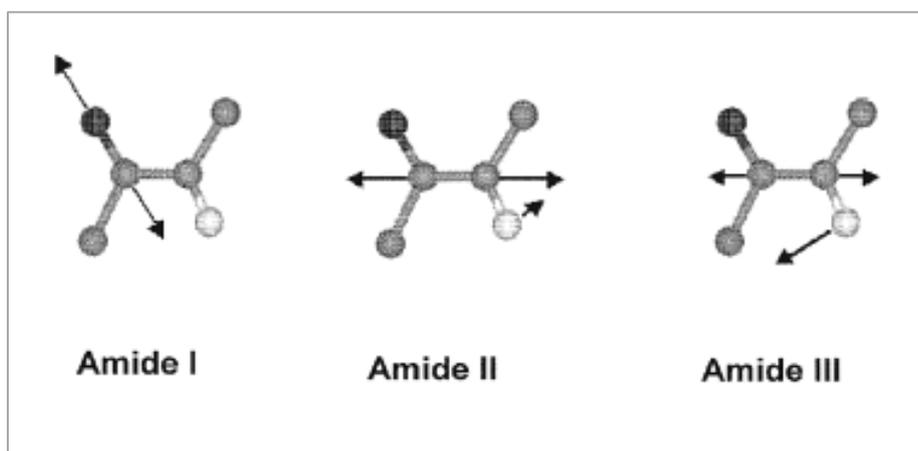
Fig 4.3: Vibrational modes for amides I, II and III (Siebert, et al., 2008).

Two major absorbance bands appeared in the second derivative spectra for free HSA as shown in (Fig. 4.4 A). These bands which are at peak positions 1656 cm^{-1} and 1546 cm^{-1} are related to the amide I and amide II bands respectively.

The absorbance spectra for HSA- Vitamin K_1 complexes with different molecular ratios of Vitamin K_1 are shown in (Figure. 4.4 B). It is clear that the absorbance intensity of HSA increases as the Vitamin K_1 molecular ratios increase; this increase in the intensity is due to the interaction between HSA and Vitamin K_1.
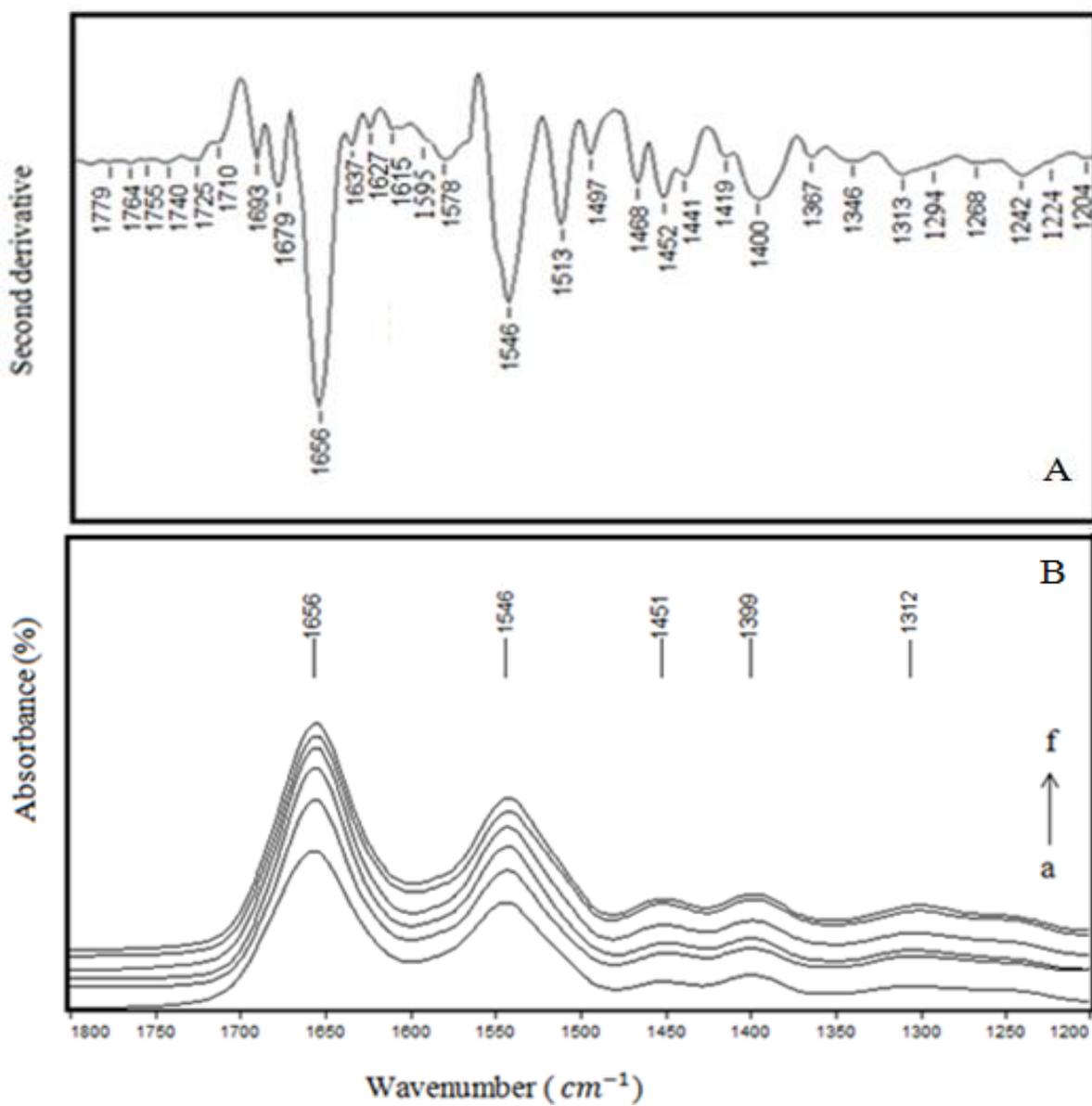
Fig 4.4: The spectra of (A): HSA free (second derivative) and (B): (a, b, c, d, e) HSA – Vitamin K_1 with molecular ratios (1:0, 1:1 1:2, 1:5, 1:10, 1:20), respectively.

The peak positions for HSA- Vitamin K_1 complexes absorption bands with different molecular ratios of Vitamin K_1 are listed in (Table 4.1). When we compare between HSA free and HSA- Vitamin K_1 complex of molecular ratio 1:20 we observe that the peak position has been shifted; For amide I band, the peak positions for HSA are shifted after mixing with Vitamin K_1 as follows: 1615 to 1613 cm^{-1}, 1627 to 1629 cm^{-1}, 1637 to 1638 cm^{-1}, 1656 to 1658 cm^{-1}, 1679 to 1682 cm^{-1}, and 1693 to 1694 cm^{-1}. For amide II region, the peak positions have been shifted as follows: 1497 to 1496 cm^{-1}, 1513 to 1514 cm^{-1}, 1546 to 1547 cm^{-1}, 1578 to 1579 cm^{-1}, and 1595 to 1593 cm^{-1}. In amide III region, the peak positions have also been shifted as follows: 1224 to 1223 cm^{-1} , 1242 to 1241 cm^{-1}, 1268 to 1269 cm^{-1}, 1294 to 1293 cm^{-1}, and 1313 to 1314 cm^{-1}.

Table 4.1: Band assignments in the absorbance spectra of HSA with different Vitamin K_1 molecular ratios for amide I, amide II, and amide III regions.

Bands	HSA Free (%)	HSA-Vitamin K_1 1:1 (%)	HSA–Vitamin K_1 1:2 (%)	HSA–Vitamin K_1 1:5 (%)	HSA–Vitamin K_1 1:10 (%)	HSA–Vitamin K_1 1:20 (%)
Amide I (1600-1700)	1615	1614	1615	1614	1614	1613
	1627	1627	1628	1628	1629	1629
	1637	1637	1637	1637	1638	1638
	1656	1656	1657	1656	1657	1658
	1679	1679	1680	1680	1681	1682
	1693	1692	1693	1693	1694	1694
Amide II (1480-1600)	1497	1497	1497	1497	1496	1496
	1513	1513	1512	1513	1513	1514
	1546	1546	1546	1547	1547	1547
	1578	1578	1579	1578	1579	1579
	1595	1595	1594	1594	1593	1593
Amide III (1220-1330)	1224	1224	1224	1224	1224	1223
	1242	1242	1441	1441	1242	1241
	1268	1268	1267	1268	1269	1269
	1294	1294	1294	1293	1293	1293
	1313	1313	1313	1312	1314	1314

The difference spectra between (HSA + Vitamin K_1) and HSA as shown in (Fig. 4.5) is performed to obtain the intensity variations result due to the interaction between HSA and Vitamin K_1. In amide I region, a strong positive peak at 1654 cm^{-1} is resulted at the lowest molecular ratio of Vitamin K_1 and at 1653 cm^{-1} at the highest molecular ratio of it. In amide II region, a weaker positive peak at 1543 cm^{-1} is resulted at the lowest molecular ratio of Vitamin K_1 and at 1542 cm^{-1} at the highest molecular ratio of it.

By comparison between the absorption spectra for free HSA which are the top two curves in (Fig.4.4) and the difference spectra of HSA and its complexes with different Vitamin K_1 molecular ratios, it is evident that the positive feature became stronger as Vitamin K_1 molecular ratio is increased with a little shift in their positions. This is related to the increase in the intensity of FTIR absorption spectra of HSA - Vitamin K_1 complexes as Vitamin K_1 molecular ratio increases which is due to the interaction between HSA and Vitamin K_1 by forming hydrogen bonds with C = O and C-N groups of the protein, and to increase of the protein α-helix structure which is also related to the interaction between HSA and Vitamin K_1 (Purcell, et al., 2000; Abu Teir., et al., 2012; N'soukpoe-Kossi, et al., 2006).
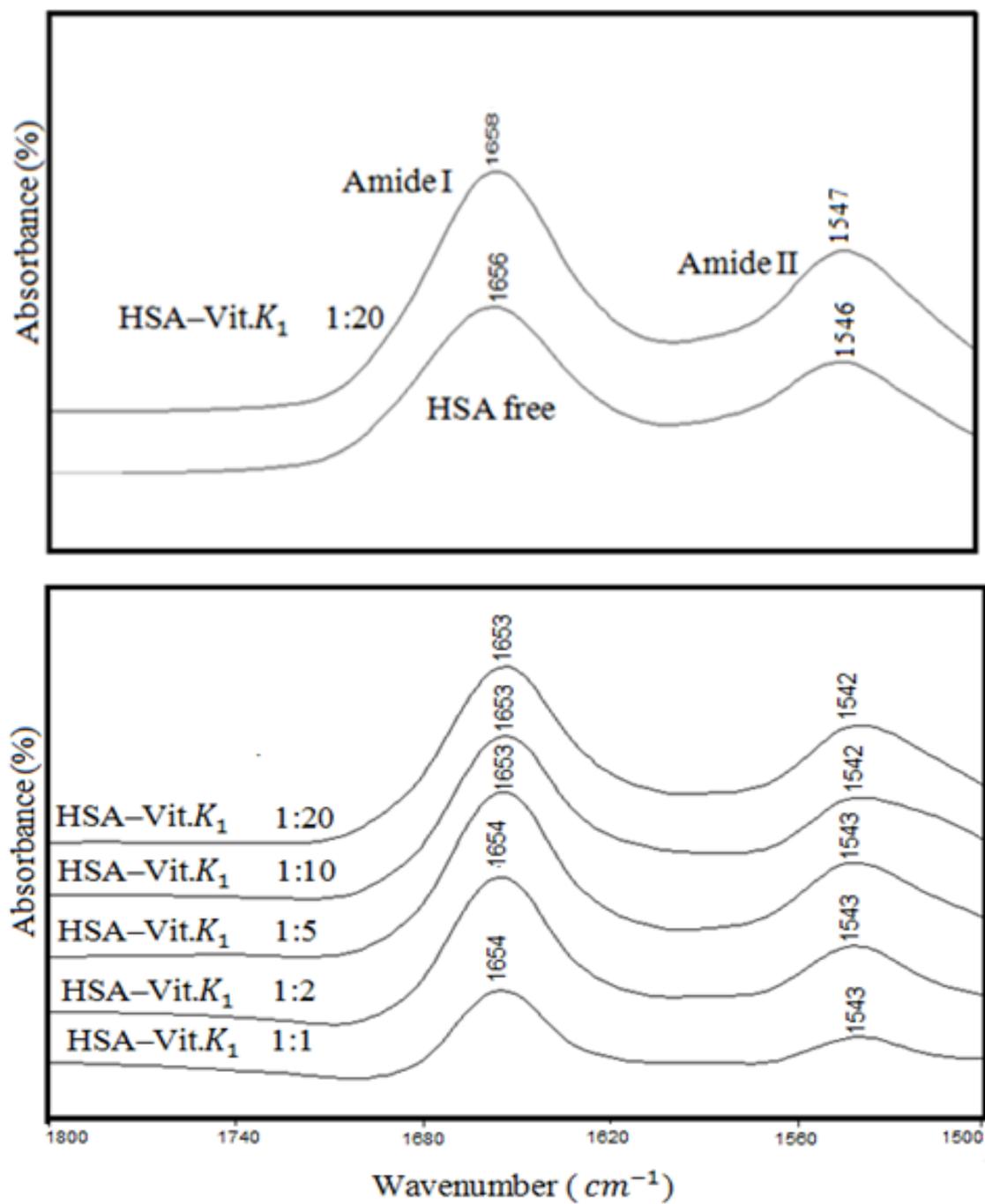
Fig 4.5: FTIR spectra (top two curves) and difference spectra of HSA and its complexes with different Vitamin K_1 molecular ratios in the region $1800 - 1500\ cm^{-1}$.

The protein amide bands have a relationship with the secondary structure of the protein (Khan, et al., 2007). The observed amide band contour of the protein consists of overlapping component bands representing different secondary structures such as α-helices, β- sheets, turns and random structures which exhibit characteristic frequencies and intensities due to the differences in the hydrogen bonds in these structures (Kong, et al., 2007; Jiang, et al., 2011).

In this work, the quantitative determination of the protein secondary structure for free HSA and HSA -Vitamin K_1 complexes in dehydrated films was performed according to the procedure described by Byler and Susi (Byler, et al., 1986).

Various data- processing techniques such as Fourier Self Deconvolution (FSD), curve fitting, and second derivative have been performed to enhance the resolution of the spectrum for the overlapping amide bands of proteins allowing the intrinsically broad components to be narrowed to estimate quantitatively the relative contributions of the different types of secondary structures (Kong, et al., 2007; Chan, et al., 2010).

The component bands of amide I, II, and III regions which are showed in (Table. 4.2) were assigned according to the frequency of its maximum appeared after baseline corrections and FSD have been applied to the absorbance spectrum. For amide I band which is in the range (1700- 1600 cm^{-1}) the ranges for the bands of the secondary structure components were assigned as follows: (1609 -1623 cm^{-1}) for β- sheets, (1623 -1647 cm^{-1}) for random coils, (1647-1672 cm^{-1}) for α- helices, (1674-1688 cm^{-1}) for turn structure, and (1688- 1700 cm^{-1}) for β- antiparallel. For amide II band which is in the range (1600- 1480 cm^{-1}) the ranges for the band components were assigned as follows: (1489-1505 cm^{-1}) for β- sheets, (1505- 1523 cm^{-1}) for random coils, (1528-1562 cm^{-1}) for α- helices, (1562- 1588 cm^{-1}) for turn structure, and (1588-1600 cm^{-1}) for β- antiparallel. For amide III which is in the range (1220- 1330 cm^{-1}), the ranges for the band components were assigned as follows: (1220-1251 cm^{-1}) for β- sheets, (1251-1288 cm^{-1}) for random coils, (1288-1297cm^{-1}) for turn structure, (1300-1330 cm^{-1}) for α- helices.

Specific areas of the protein secondary structures are needed to be calculated for quantitation of the respective absorbance, or for a comparative analysis. For a deconvolved spectrum, the peak area assessment signifies a summation of all the absorbance values over the wavenumber range in which the band show up by means of integration (Severcan, et al., 2012), then the absorbance percentages of each secondary structure were calculated by dividing the integrated area for each component by the total area of the amide band. The absorbance percentages of each secondary structure for free HSA and for HSA -Vitamin K_1 complexes in amides I, II, and III are listed in (Table. 4.2).

The second derivative and curve fitting was performed on the absorption spectra for HSA free and the HSA- Vitamin K_1 of highest molecular ratio as shown in (Fig. 4.6). It is clearly observed that the percentages of α- helices increases, whereas the percentages of β- sheets decreases as the molar ratios of Vitamin K_1 increase in all the amide regions (I, II and III). The increase of percentage absorbance intensity resulted from α- helices intensity in favor of the reduction of that for β- sheets-which indicates that Vitamin K_1 interacts with HAS-is related to the partial unfolding of the protein in the presence of Vitamin K_1 as a result of the formation of H- bond between the c=o of Vitamin K_1 and the hydrogen of the amino group in the peptide bond which effects the electron flow between the nitrogen and the carbon atom of the carboxyl group of the peptide, so the C = O in the carboxyl of the peptide assumes a partial double bond which decrease percentage absorbance intensity resulted from β- sheets, so the percentage absorbance intensity resulted from α- helices.

Table 4.2: Secondary structure determination for amide I, amide II, and amide III regions in HSA and its Vitamin K_1 complexes.

2nd structure	HSA Free (%)	HSA – VitaminK$_1$ 1:1 (%)	HSA – Vitamin K$_1$ 1:2 (%)	HSA – Vitamin K$_1$ 1:5 (%)	HSA – Vitamin K$_1$ 1:10 (%)	HSA – Vitamin K$_1$ 1:20 (%)
			Amide I			
β-sheets (cm^{-1}) (1609-1623) (1688-1700)	20	19	18	16	16	15
Random (cm^{-1}) (1623-1647)	10	11	12	12	13	13
α-helix (cm^{-1}) (1647-1672)	56	57	58	58	58	59
Turn (cm^{-1}) (1674-1688)	14	13	12	12	11	11
			Amide II			
β-sheets (cm^{-1}) (1489-1505) (1588-1600)	22	22	21	20	20	19
Random (cm^{-1}) (1505- 1523)	10	10	10	11	12	13
α-helix (cm^{-1}) (1528-1562)	53	53	54	55	55	56
Turn (cm^{-1}) (1562-1588)	15	15	15	14	13	12
			Amide III			
β-sheets (cm^{-1}) (1220-1251)	20	20	19	19	19	18
Random (cm^{-1}) (1251-1288)	16	16	16	17	17	17
Turn (cm^{-1}) (1288-1297)	11	11	11	10	10	10
α-helix (cm^{-1}) (1300-1330)	50	50	51	51	51	52

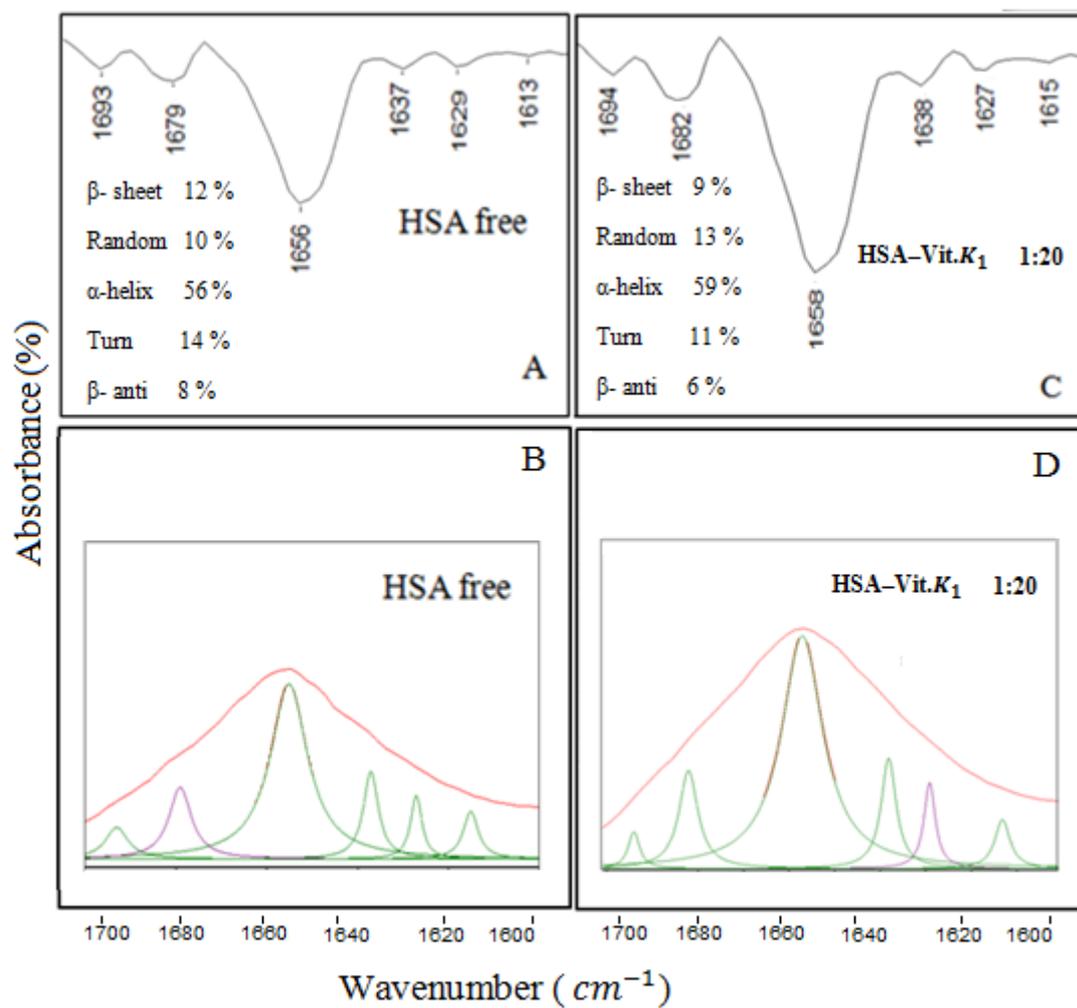**Fig 4.6**: Second derivative resolution and curve fitted amide I region (1700-1600 cm^{-1}) and secondary structure determination of the free HSA (A, B) and its Vitamin K_1 complexes (C, D) with 1:20 protein: vitamin ratio.

Chapter Five

Conclusions and Future work

Chapter Five

Conclusion and Future work:

5.1 Conclusion

The interaction of HSA with Vitamin K_1 is Almost similar to the interaction of it with the Vitamin A components (retinol and retinoic acid) according to the published article (N'soukpoe-Kossi, et al., 2007), whereas, it is almost differ from the interaction between it with Vitamin D and Vitamin E (Abu Teir, Abu-hadid, Abu Awwad, Personal communications) .

Using UV-Vis absorption spectrophotometry, I found that the value of the binding constant between HSA and Vitamin K_1 equals 60 M^{-1}, this value indicates a weak binding between them in comparison with other hydrophobic vitamins which have binding constants with values 1.32×10^5 M^{-1}, 3.33×10^5 M^{-1}, 1.21×10^2 M^{-1}, 6.8×10^1 M^{-1} for retinol, retinoic acid, Vitamin E and Vitamin D respectively (N'soukpoe-Kossi, et al., 2007; Abu Teir, Abu-hadid, Abu Awwad, Personal communications).

FTIR spectroscopy data indicated that the absorbance intensity increases as the molecular ratios of Vitamin K_1 increase, this increase in intensity is related to the increase of the absorbance intensity for α- helices which indicated that the interaction between HSA and Vitamin K_1 leads to the folding of the protein by forming new H- bonding in the C = O bond assuming partial double bond character due to a flow of electrons from C − N to C = O bond which increases the intensity of the absorbance of the α- helices. This increase in the intensity is similar to the increase observed of the interaction between Vitamin A components (retinol and retinoic acid) and HSA, but with different absorbance ratios (N'soukpoe-Kossi, et al., 2007).

5.2 Future Work

Studying the interaction between HSA and Vitamin K_1 is very important due to the great importance of the binding between them in the body distribution of the vitamin. Further studies can be done about the temperature dependence of the vitamin interaction with HSA. Furthermore, determination of the thermodynamic parameters such as enthalpy and free energy at different temperatures can be studied to investigate the type of the forces acting for the binding between them.

References

Abu Teir, M. M., Githan, J., Darwish, S., Abu-hadid, M. M. (2012). Journal of Applied Biological Science 6, 3, 45-55.

Banwell, C. N. (1972): Fundamentals of Molecular Spectroscopy. 2 nd ed. McGraw-Hill Book Company (UK) Limited.

Barth, A., Haris, P. I. (2009): Advances in Biomedical Spectroscopy: Biological and Biomedical Infrared Spectroscopy. Tha authers and IOs Press.

Benzakour, O. (2008). Thromb Haemost 100, p527.

Bernath, P. F. (2005): Spectra of Atoms and Molecules. 2 nd ed. Oxford University Press. Inc.

Branden, C., Tooze, J. (1999): Introduction to Protein Structure. 2 nd ed. Garland Puplishing, Inc.

Byler, D. M., Susi, H. (1986). Biopolymers 25, 469-487.

Champe, P. C., Harvey, R. A. (1994): Lippincott's Illustrated Reviews: Biochemistry. 2 nd ed. J. B. Lippincott – Raven.

Chan, E.C., Griifiths, P. R., Chalmers, J. M. (2010): Applications of Vibrational Spectroscopy in Food Science. John Wiley & Sons, Ltd.

Coats, J. (2000): Interpretation of Infrared Spectra, A Practical Approach. John Wiley & Sons, Ltd.

Campell, N. A. (1996): Biology. 4 th ed. John Seton.

Campell, N. A., Reece, J. B., Urry, L. A., Cain, M. L., Wasserman, S. A., Minorsky, P. V., Jackson, R. B. (2008): Biology. 8 th ed. Pearson Education, Inc.

Combs, G. F. (2008): The Vitamins: Fundamental Aspects in Nutrition and Health. 3 rd ed. Elsevier Academic Press.

Damon, M., Zhang, N. Z., Haytowitz, D. B., Booth, S. L. (2005). Journal of Food Composition and Analysis 18, p751.

Darwish, S. M., Abu Sharkh, S. E., Abu Teir, M. M., Makharza, S. A. (2010). Journal of Molecular Structure 963, 122-129.

Delvin, T. M. (1997): Text Book of Biochemistry with Clinical Correlations. John Wiley & Sons, Inc.

Derrick, M. R., Stulik, D., Landry, J. M. (1999): Infrared Spectroscopy in Conservation Science. The J. Paul Getty Trust.

Ewen, S., Dent, G. (2005): Modern Raman Spectroscopy: Appractical Approach. John Wiley & Sons, Ltd.

Fale, P. L., Ascensao, L., Serralherio, M. L., Haris, P. I. (2011). Spectroscopy 26, 79-92.

Friedrich, W. (1988): Vitamins. Walter de Gruyter.

Gregoriou, V. G., Braiman, M. S. (2006): Vibrational Spectroscopy of Biological and Polymeric Materials. Taylor & Francis Group, LLC.

Griffiths, P. R. (2007): Fourier Transform Infrared Spectrometry, 2 nd ed. John Wiley & Sons, Inc.

Grooper, S. S., Groff,Smith, J. L., Groff, J. L. (2009): Advanced Nutrition And Human Metabolism. 5 th ed. Wadsworth, Cengage Learning.

Gupta, M. C. (2001): Atomic and Molecular Spectroscopy. New Age International (P) Ltd.

He, X. M., Carter, D. C. (1992). Nature 358, p209.

Hou, H. N., Qi, Z. D., Ou Yang, Y. W., Liao, F. L., Zhang, Y., Liu, Y. (2008). Journal of Pharmaceutical and Biomedical analysis 47, 134-139.

IFS 66v/S user's manual. (1998). BRUKER OPTIC GmbH.
Jiang, Y., Li, C., Nguyen, X., Muzammil, S., Towers, E., Gabrielson, J., Narhi, L. (2011). Journal of Pharmaceutical Science 100, 11.

Karnaukhova, E. (2007). Biochemical Pharmacology 73, p901.

Kauppinen, J., Partanen, J. (2001): Fourier Transforms in Spectroscopy. Wiley-VCH Verlage GmbH.

Khan, S. N., Islam, B., Khan, A. U. 92007). International Journal of Integrative Biology (IJIB) 1, 2, p102.

Kong, J., Yu, S. (2007). Acta Biochimica et Biophysica Sinica 39, 8, 549-559.

Kragh-Hansen, U., Chuang, V. T., Otagiri, M. (2002). Biol. Pharm. Bull 25, p701.

Larkin, P. J. (2011): Infrared And Raman Spectroscopy: Principles And Spectral Interpretation. Elsevier Inc.

Levine, I. N. (1975): Molecular Spectroscopy. John Wiley & Sons, Inc.

Lusi, J., Arrondo, R., Goni, F. M. (1999). Progress in Biophysics & Molecular Biology 72, p367.

McLean, L. R., Pelton, J. T. (2000). Analytical Biochemistry 277, 167-176.

McMurry, J. (1990): Fundamentals of Organic Chemistry. Wadsworth, Inc.

Michael Hollas, J. (2002): Basic Atomic and Molecular Spectroscopy. The royal Society of Chemistry.

Michael Hollas, J. (2004): Modern Spectroscopy. 4 th ed. John Wiley & Sons, Ltd.

Nakamoto, K. (1978): Infrared and Raman Spectra of Inorganic and Coordination Compounds. 3 rd ed. John Wiley & Sons, Inc.

NanoDrop (ND − 1000) spectrophotometer Version 2.5 User's Manual. (2006). NanoDrop Technologies, Lnc.

Nikolic, G. S. (2001): Fourier Transforms-New Analytical Approach and FTIR Strategies. InTech.

N'soukpoe-Kossi, C. N., Sedaghat-Herati, R., Ragi, C., Hotchandani, S., Tajmir-Riahi, H. A. (2007). International Journal of Biological Macromolecules 40, 484-490.

Ohannesian, L., Streeter, A. J. (2002): Handbook of Pharmaceutical Analysis. Marcel Dekker, Inc.

OPUS Bruker manual version 5.5. (2004): BRUKER OPTIC GmbH.

Ouameur, A. A., Mangier, E., Diamantoglou, S., Rouillon, R., Carpentier, R., Tajmir-Riahi, H. A. (2004). Biopolymers 73, p503.

Ouameur, A. A., Marty, R., Tajmir-Riahi, H. A. (2005). Biopolymers 77, 129-136.

Pavia, D. L., L., Lampman, C. M., Kriz, G. S. (2001): Introduction to Spectroscopy. 3 rd ed. Thomson Learning, Inc.

Petereson, J. W., Muzzey, K. L., Haytowitz, D., Exler, J., Lemar. L., Booth, S. L. (2002). JAOCS 79, 7, p641.

Purcell,M., Neault, J. F., Tajmir-Riahi, H. A. (2000). Biochimica et Biophysica Acta 1478, 61-68.

Sathyanarayana, D. N. (2004): Vibrational Spectroscopy: Theory and Applications. New Age International (P) Ltd.

Severcan, F., Haris, P. I. (2012): Vibrational Spectroscopy Diagnosis and Screening. The authers and IOs Press.

Sibert, F., Hildebrant, P. (2008): Vibrational Spectroscopy in Life Science. WILEY-VCH Verlage GmbH & co. KGaA, Weinheim.

Smith, B. C. (1996): Fundamentals of Fourier Transform Infrared Spectroscopy. CRC Press LLC.
Stan, D., Matei, I., Mihailescu, C., Savin, M., Matache, M., Hillebrand, M., Baciu, I. (2009). Molecules 14, p1615.

Steele, D. (1971): The Interpretation of Vibrational Spectra. Barnes & Nobel, Inc.

Stuart, B. H. (1997): Biological Applications of Infrared Spectroscopy. John Wiley & Sons, Ltd.

Stuart, B. H. (2004): Infrared Spectroscopy: Fundamentals and applications. John Wiley & Sons, Ltd.

Suttie, J. W., Mummah-Schendel, L. L., Shah, D. V., Lyle, B. J., Greger, J. L. (1988). Am J Clin Nutr 47, p475.

Svanberg, S. (2004): Atomic and Molecular Spectroscopy: Basic Aspects and Practical Applications. 4 th ed. Hiedelberg New York.

Tajmir-Riahi, H. A. (2006). Journal of The Iranian Chemical Society 3(4), 297- 304.

Tajmir_Riahi, H. A. (2007). Scientia Irania 14 (2), 87-95.

Tavirani, M. R., Moghaddamnia, S. H., Ranjbar, B., Namaki, S., Zolfaghari, P. (2005). Iranian Journal of Pharmaceutical Research 4, p240.

Thane, C. W., Bates, V. J., Shearer, M. J., Unadkat, N., Harrington, D. J., Paul, A. A., Prentice, A., Bolton-Smith, C. (2002). British Journal of Nutrition 87, p615.

Tian, J., Chen, C., Xue, M. (2011). Spectroscopy 26, p195.
Tuan, V., Chuang, G., Otagiri, M. (2001). Biochemica et Biophysica Acta 1546, p337.

Usui, Y., Tanimura, H., Nishimura, N., Kobayashi, N., Okanoue, T., Ozawa, K. (1990). Am J Clin Nutr 51, p846.

Valeur, B. (2001): Molecular Fluorescence: Principles and Applications. Wiley-VCH Verlag GmbH.

Wang, T., Xiang, B., wang, Y., Chen, C., Dong, Y., Fang, H., Wang, M. (2008). Colloids and Surfaces B: Biointerfaces 65, p113.

Wartewig, S. (2003): IR and Raman Spectroscopy: Fundamental Processing. WILEY-VCH verlag GmbH & Co. KGaA, Weinheim.

الملخص

ان عمليات الامتصاص و التوزيع وعمليات الايض التابعة للعديد من الجزيئات يمكن ان يحدث فيها تغيير بالاعتماد على ميلها للارتباط ببروتين الدم البشري (Human Serum Albumin). ان بروتين الدم البشري عادة يزيد ذائبية المواد الموجودة في البلازما ويعدل طريقة نقلها الى الخلايا. في هذه الدراسة تم دراسة الارتباط بين فيتامين K_1 وبروتين الدم البشري باستخدام جهاز مطياف الأشعة فوق البنفسجية (UV-Vis spectrophotometer) وجهاز مطياف تحويل فورير للأشعة الحمراء (Fourier Transform Infrared spectrometer). وتم معرفة قيمة ثابت الارتباط والتأثير على البناء الثانوي للبروتين. عند استخدام جهاز مطياف الأشعة فوق البنفسجية لدراسة الارتباط بين فيتامين K_1 وبروتين الدم البشري، ولوحظ ان شدة امتصاص الأشعة فوق البنفسجية (Maximum Intensity) لبروتين الدم مع الفيتامين تزداد بازدياد تركيز الفيتامين في المخلوطات التي تحتوي على تركيز ثابت من البروتين وتراكيز مختلفة من الفيتامين. ومن خلال هذه النتائج تم حساب ثابت الارتباط بين الفيتامين وبروتين الدم البشري ووجد ان قيمته هي $60\ M^{-1}$.

وعند استخدام جهاز مطياف تحويل فورير للأشعة الحمراء (FTIR)، ووجدنا ان شدة امتصاص الأشعة الحمراء تزداد بازدياد تركيز الفيتامين مع بقاء تركيز البروتين ثابت. ومن خلال بعض التقنيات مثل (Second derivative)، (BaseLine correction)، (Fourier self deconvolution) وال (Curve fitting) تم تحديد التغيرات التي حصلت على البنية الثانوية للبروتين في مناطق الأميد الأول والأميد الثاني والأميد الثالث، حيث وجد أن هناك تغيرات في مواقع بعض القمم عندما تغيير تركيز الفيتامين ولوحظ ايضا ان نسبة شدة الامتصاص الناتجة عن (α-helix) تزداد بازدياد تركيز الفيتامين على حساب نسبة شدة الامتصاص الناتج عن (β- sheets). هذه التغيرات ناتجة عن التفاعل بين فيتامين K_1 وبروتين الدم البشري عن طريق تكوين روابط هيدروجينية جديدة بين البروتين والفيتامين.